Network modeling and behavioral characterization of *Hydra* contraction dynamics

A Thesis

submitted to

Indian Institute of Science Education and Research Pune

the partial fulfilment of the requirements for the

BS-MS dual degree programme

by

Divyansh Gupta

Indian Institute of Science Education and Research, Pune

Dr. Homi Bhabha Road,

Pashan, Pune 411008, India

Supervisor: Adrienne Fairhall

May 2024

Certificate

This is to certify that this dissertation entitled **Network modeling and behavioral characterization of *Hydra* contraction dynamics** submitted towards the partial fulfillment of the BS-MS degree at the Indian Institute of Science Education and Research, Pune represents original research carried out by Divyansh Gupta at Computational Neuroscience Center, University of Washington, under the supervision of Dr Adrienne Fairhall during academic year May 2023 to Mar 2024.

Supervisor:
Dr Adrienne Fairhall
Professor of Physiology and Biophysics
University of Washington

Divyansh Gupta
20191007
BS-MS
IISER Pune

Thesis Advisory Committee:
Dr Collins Assisi
Assistant Professor, Biology
Indian Institute of Science Education and Research, Pune

Declaration

I, hereby declare that the matter embodied in the report titled **Network modeling and behavioral characterization of *Hydra* contraction dynamics** is the result of the investigations carried out by me at the Computational Neuroscience Center, University of Washington from the period May 2023 to Mar 2024 under the supervision of Prof Adrienne Fairhall and the same has not been submitted elsewhere for any other degree.

Divyansh Gupta
IISER Roll No: 20191007
Date: 27th March 2024

Acknowledgements

First, I would like to thank my supervisor Dr Adrienne Fairhall for her mentorship and constant encouragement, and Hengji Wang, who built the hydra model and taught me how to assess data and make sense of it. I also want to thank members of the Fairhall Lab and the CNC community, and in particular Scott Sterrett, Alison Duffy, Patrick Zhang, David Bell, Po-chen Kuo, Ilse Dippenair, Vaibhav Thakur, Faeze Amimanasoor, John Ferre, Fereshteh Lagzi, Vyom Raval, Srinidhi Naidu for their advice and friendship.

I would like to thank Vasudha who has been the one constant source of support and love. I'm also grateful for my friends Aditya, Neev, Garvit, Varun, Amogh Ranade, Aniketh, Amogh Rakesh, and Vatsal.

I would also like to thank Dr Collins Assisi and Dr Suhita Nadkarni for their continuing mentorship and support. I would also like to thank members of the computational neuroscience group at IISER for their friendship and support. I would also like to acknowledge the late KVPY programme for the opportunity of attending IISER Pune.

Finally I want to thank my parents and my sister for their support.

Abstract

Hydra is a cnidarian possessing some of the earliest extant nervous systems comprising of nerve nets of diffusely spread neurons that coordinate its behavior without any centralization. It is also a well studied model organism in developmental biology for its remarkable ability to regenerate. With its simple nervous system it exhibits a behavioral repertoire comprising of spontaneous contractions and multi-step whole-body coordinated behaviors like somersaulting and prey-capture for feeding. How the nerve net of *Hydra* orchestrates these movements is not understood. Recent advances in genomics and calcium imaging allow for unprecedented insights into large scale neural recordings, the size of hydra also makes it particularly appealing for complete observations of neural activity and behavior.

Using a two population network model driven by mechanosensitivity incorporating gap junctions and mutual inhibition we model the neural activity that controls these spontaneous contractions and put together ideas about the neurophysiology of *Hydra* into a coherent mechanistic model. I extract neural activity and behavior from a dataset comprising of calcium imaging videos of freely behaving animals in a petri-dish before being bisected, into two halves which were then imaged separately over the course of regeneration, and use these to constrain and validate the model.

I show that this model captures the switching of activity between the sub-networks and the recovery of the contraction behaviour after bisection, but misses higher order variation in the activity which might be light-driven or affected by many other sources of variability in the animal's neural circuitry including interactions with other sub-networks, neuropeptides and a stochastic water influx. This model could serve as the basis for future work incorporating more detail from *Hydra* neurophysiology as it gets discovered and provide a more comprehensive understanding of the hydra nervous system.

Contents

List of Figures

Chapter 1

Introduction

Hydra belongs to the phylum Cnidaria which comprises some of the earliest forms of extant nervous systems [1–3]. Nervous systems likely first emerged in the common ancestor of cnidarians and bilaterans, of which we and all other mammals are a part. These nerve nets are composed of neurons diffusely spread across the body of the animal without any apparent centralization. *Hydra* has become an important model organism in developmental biology due to its unique ability to regenerate after being cut into pieces, or even diassociated into individual cells [4].

Previous work in *Hydra* largely consists of behavioral and electrophysiological recordings using single electrodes placed near a stationarized hydra [5–7]. These experiments have led to interesting insights about the constitution of the nervous system and the subnetworks that might be giving rise to the specific neural activity observed. Recent genomics advances in *Hydra*, including the sequencing of the complete genome of the animal [8], characterization of stem cell lineages [9] and the development of transgenic lines that allow for imaging of whole body neural & muscular imaging alongside behavioral observations promise exciting progress in understanding its neurobiology [10, 11].

1.1 Body plan

Hydra possesses a radially symmetric body plan consisting of two germlayers, the ectoderm and the endoderm, with an acellular mesoglea in between them [3]. It has tentacles located at the hypostome (near the mouth) and it attaches itself to its substrate through specialized cells in the peduncle (basal region). The tentacles possess cnidocytes, which are stinging cells, part of a battery cell complex that has both sensory and effector cells it uses to detect and paralyse prey.

The ectoderm consists of longitudinally oriented muscles while the muscles of the endoderm are radially oriented. The mouth of the animal is located near the base of the tentacles, which is sealed and is opened through a forceful tearing between the cells for

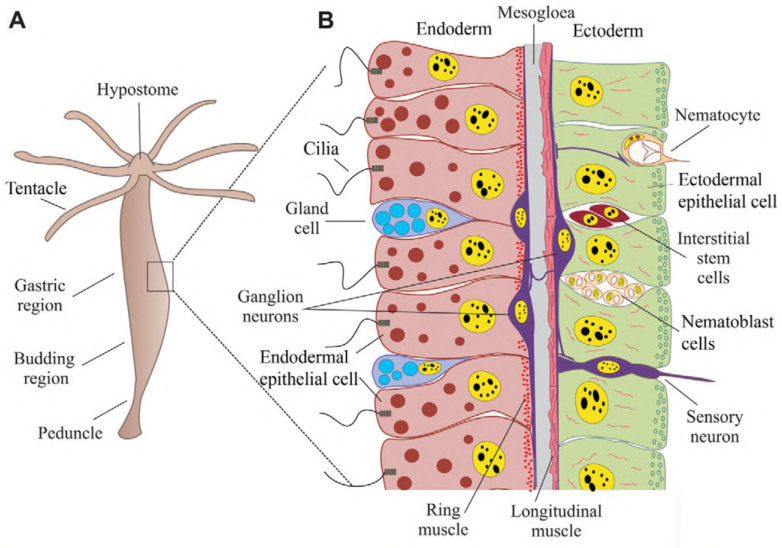

Fig. 1.1. *Hydra* body plan showing the two germ cell layers along with the acellular mesoglea. The two layers possess two independent nerve nets comprising of multiple ensembles along with epitheliomuscular cells and other specialized cells. (Adapted from Technau & Steele, 2011 [3]).

each spontaneous contraction [12].

1.2 Behavior

Hydra shows a repertoire of behavior that includes spontaneous contractions, bending, tentacle swaying, feeding and somersaulting [13]. It also exhibits sleep-like behavior [14]. Its contractions and somersaulting show diurnal variation which also depend on the hunger state of the animal [6]. Somersaulting is the primary way that the animal locomotes; it exhibits phototaxis through somersaulting towards light. *Hydra*'s heliotropism has also been noted for a long time [15].

The spontaneous contractions of *Hydra* have puzzled scientists for some time. The animal alternates between periods of elongation and the contraction burst which comprise of discrete pulses of whole body contractions during which the mouth of the animal ruptures open and expels out water [12, 16]. The contractions occur spontaneously without any apparent external stimulus to the animal. These contractions are also known to be affected by mechanical agitation and light stimulus [6, 17]. The animal also shows spontaneous bending behavior. That has been linked with asymmetrical calcium waves in the ectodermal muscular network [18]. Bending also occurs as an element of the longer mutli-step coordinated movement the animal exhibits, the somersault.

Hydra's feeding behavior follows a stereotypical pattern of body movements. The sequence comprises of tentacle writhing, tentacle ball formation and mouth opening [19]. Food associated molecules such as reduced glutathione (GSH) can be used to induce

the feeding response [20].

Hydra locomotes through somersaulting, which comprises a series of steps that form a fixed action pattern, i.e. that once initiated the animal undergoes the full sequence in the same order [21]. The sequence consists of elongation, tentacle attachment to the substrate, basal disc detachment, contraction, elongation, basal disc reattachment, and tentacle detachment. It has also been shown that somersaulting towards light is satiety dependent [22], with starved hydra showing a higher frequency of somersaulting towards light. Somersaulting is driven by the peptide Hym-248 which is expressed in the neurons of the RP network [21]. A bath application of the peptide increases the somersaulting frequency. A key event in the fixed action pattern associated with the neural activity is a linear ramp of RP network firing frequency which then explodes just before the basal disc detachment.

Recent advances in computer vision and deep learning have led to the development of tools for tracking animal pose and movement with high resolution [23]. DeepLabCut is one of the most popular of such tools [24]. It relies on transfer learning and allows for pose-estimation without markers using keypoints labeled on a small subset of video frames by the experimenter. Using such digital tracking of animal movement and reducing the dimensionality of animal behavior through dimensionality reduction methods such as PCA, animal behavior can be characterized as trajectories through postural space. Unsupervised discovery of such trajectories allows for segmentation of behavior that is not dependent on an anthropocentric gaze [25].

1.3 Neurophysiology of *Hydra*

Earlier neurophysiological investigations on *Hydra* relied on single electrodes placed close to or in contact with the body of a pinned down animal preparation. Passano & McCulloch through their extensive electrophysiological recordings of a pinned *Hydra* found that there are multiple nerve nets which give rise to different activity [5–7]. There is evidence for both electrical and chemical synaptic transmission in the *Hydra* based on electron microscopy driven observations of dense core vesicles [26].

The neural activity they recorded could be classified in two regimes, a burst of large sweeps in recorded electrical potential, which coincided with contractions of the animal body, and regimes of elongation where the recorded neural activity showed small amplitude oscillations. They found that the subnetwork responsible for giving rise to the contractions has its pacemaker neurons in the hypostome and called it the contraction burst (CB) network. There is another subnetwork that gives rise to the smaller-amplitude rhythmic potentials, and is called the RP network. The whole animal's neural activity recording through a nearby electrode presents an alternating pattern of firing between the rhythmic potentials and the contraction bursts.

Recent advances in applications of genomics and calcium imaging to *Hydra* have allowed unprecedented insight into the network activity of the animal while it is freely engaging in behavior. Using these advances, *Hydra* lines expressing calcium indicators have been

established and it is found that there are multiple non-overlapping nerve nets in the body of the animal [10]. The CB and RP1 subnetworks were found to be localized in the ectodermal layer, along with the tentacular subnetwork, while a second quasi-rhythmically firing subnetwork, which Dupre & Yuste called 'RP 2', is localized in the endoderm. The activity of the CB and the ectodermal RP network is strongly anti-correlated, suggesting that they may mutually inhibit one another.

Hydra was long supposed to possess gap junctions based connections in its nerve nets due to the synchronous nature of firing of its sub-networks. Through electron microscopy, the presence of gap junctions was established, which has been recently confirmed more extensively based on analysis of the *Hydra* genome [8] for the presence of innexins, gap junction forming proteins. But the presence of innexins in itself isn't conclusive proof of formation of functional gap junctional channels. In 2014, Takaku and others showed via antibody-staining based methods that there are functional gap junctional channels in the nerve net at the peduncular region [27].

Through clever experiments involving cutting the body of the animal across different axes, the presence of connections along different directions has been tested [6, 7, 28]. These studies have also lent insight into the spatial organization of different components of the nerve nets in *Hydra*. Passano & McCulloch showed that *Hydra* with their hypostomes removed do not show contractions until they regenerate, suggesting that neurons with pacemaker-like properties in the CB subnetwork are localized to the hypostome. Similarly neurons in the RP subnetwork with pacemaker properties were found to be more diffusely spread across the body column of the animal with a high density in the peduncular ring.

Kass-Simon showed that connections in the animal body are more prominent along the vertical axis than in the horizontal axis [28]. They did this by making hydra preparations into I and H shapes and injecting current on one end of the animal with an electrode and detecting it at the other end of the animal. The cut ensured that propagation of electrical activity could only occur in either the vertical or the horizontal direction in the two preparations respectively.

The role of the nervous system in coordinating all *Hydra* behavior has been established beyond doubt. Artificially denervated hydra have been shown to lose all ability to move and feed. They also lose the spontaneous contractions [29]. Though they retain the ability to contract when poked which might suggest a mechanosensory component to the epitheliomuscular cells too.

1.4 Mechanosensitivity & osmoregulation

Hydra also exhibits a well-characterized mechanosensory response. It contracts immediately in response to touch [17] and this response exhibits habituation if done repeatedly. Since *Hydra* lives in freshwater environments, it faces the challenge of osmoregulation that most freshwater organisms do, i.e. the environment is hypo-osmotic with respect to the extracellular space of the animal's body and water is constantly absorbed. It has

been established that there are extracellular vacuoles in the animal's body that contain high concentrations of sodium, potassium and other ions [30]. There is an overall gradient from the extracellular space in an animal's body to its lumen, with the lumen having lower osmolarity than the extracellular space but higher than the external freshwater environment.

It has been suggested that this osmotically driven water influx in the animal body may be the primary driver of the spontaneous contractions, which would then serve the purpose of periodically expelling out excess water collected in the animal's lumen [31].

1.5 Light sensitivity

Hydra has been long known to exhibit phototaxis. The response of the nerve nets to light in experimental settings varies depending on both the properties of the light stimulus and the phase of the network activity of the animal. These stimulus properties include the duration, the localization extent, the wavelength and the amplitude variation of the light stimulus [32–35]. Blue light drives the peak of the photoresponse of the animal, and red light effectively ellicits no response [6, 7].

The mechanism underlying light modulation of neural activity and behavior in *Hydra*, along with most cnidarians, relies on extraocular photosensitivity, i.e. photosensitivity without ocular or eye-like specialized structures consisting of multiple cell types. Recent genomic and transcriptomic analyses have shown that the expression of opsins and other proteins involved in phototransduction cascades is most prominent in the tentacles [36–38].

Broadly, the RP network firing frequency increases when a localized or a whole body light stimulus is applied to the animal. If the stimulus onset, either of illumination of the whole animal or a localized region near the hypostome, occurs during an undergoing contraction burst, the burst halts. It has been suggested that this is the effect of an abruption and a shifting of the effective pacemaker locus [6]. The contraction burst frequency also shows diurnal-like variations, where they decrease just before dawn, and then increase again [6, 32].

When the whole animal is stimulated at different times within its contraction elongation cycle, the phase of its cycle is shifted [33]. When stimulated early in the cycle (during a contraction), the contraction halts and the succeeding contraction occurs earlier than it would have without any stimulation, resulting in a 'phase advance'. When the network is stimulated later in the cycle, during elongation, the next contraction occurs later than it would have, causing a 'phase delay'.

1.6 Regeneration

Hydra exhibits unique regenerative capabilities that make it an excellent model system for developmental biology and stem cell research. When the animal is cut anywhere

along the vertical axis, the two halves develop into two full animals. And when the animal is chemically dissociated down to the cellular level by centrifugation and allowed to reaggregate, the clump of cells coalesce and reorganize into a fully functional animal [4]. This regenerative ability also makes *Hydra* a fascinating neuroscientific model organism to study how network activity in the animal recovers when the spatially organized subnetworks are separated from each other.

In this thesis, we will look at a dataset comprising of calcium imaging videos of the regenerating animal after being bisected in two halves via a horizontal cut at the center of the midline. Through an analysis of the neural activity over regeneration we will study recovery of neural circuitry and behavior in bisected hydra.

1.7 What we did

There is a paucity of modeling work that explains cohesively the various facts known about hydra and cnidarian neurophysiology (as illustrated in the above sections). Our goal in this thesis is to build a neural model of contraction dynamics in *Hydra*. A key contribution of this work is an analysis of a unique data set assembled by Joshua Swore [39], consisting of videos of freely behaving whole and bisected transgenic hydra animals, imaged using calcium indicators (GCaMP6s) expressed in their nerve nets. Using image processing and spike detection methods, I used this dataset to extract neural activity from the animal's body and classify it as arising from either of the two pre-dominant subnetworks. This analysis provides an insight into network activity in the animal's body as it undergoes regeneration, and serves as an important constraint for our network modeling.

Our mechanistic model combines ideas of mechanosensitivity, gap junctional synchronization, mutual inhibition between the subnetworks and pacemaker organization to explain network activity in *Hydra*, with its characteristic alternation between rhythmic potentials and contraction bursts. The model explains the different activity patterns observed in the two halves of the animal upon bisection and the changes as each undergoes regeneration, including an account of the recovery of circuit activity as more neurons with pacemaker-like properties are added over the course of regeneration.

In the neural activity of these regenerating animals we see patterns and variation that our model, relying on a uniform osmotic drive, doesn't capture. Using ideas from *Hydra* electrophysiology literature and light sensitivity I suggest expansions of the model that might explain this variation. These ideas about light driven excitation and stochasticity of activity switching can be better constrained with more directed future experiments.

I also extracted the behavior of the animal from these videos using pose-estimation based on deeplabcut. This allows us to also estimate the length of the animal which corroborates our classification of neural activity underlying spontaneous contractions. Via interpolation between the tracked keypoints we extract the shape of the midline of the animal over these videos of the whole animal and bisected regenerating halves showing graceful movements and structure in the bisected animals as they recover their

movement behavior, which presents an interesting future direction to investigate the control of postural dynamics in *Hydra*.

Chapter 2

Model

The basis of the network model advanced in this work was developed by Hengji Wang as a part of his PhD thesis titled "Modeling Hydra from muscle to neuron to behavior" [40].

2.1 Neuron model & Mechanosensitivity

The model consists of two populations of neurons, corresponding to the Rhythmic Potential (RP) and Contraction Burst (CB) networks. Single neurons are modeled as canonical leaky integrate and fire neurons with input from a mechanosensitive current.

$$\frac{dV}{dt} = -\frac{1}{C_m}[I_s + g_L(V - E_l)] \tag{2.1}$$

Here V is the membrane potential, C_m is the capacitance, I_s is the mechanosensitive inward current, g_L is the leak conductance and E_l is the resting membrane potential.

The mechanosensitive ion channels are modeled as Piezo channels which are found to be expressed in most neurons (and other cell types) in Hydra [9]. We model them with a form based on known crustacean stretch receptors. The inward flux from the Piezo ion channels is modeled as:

$$I_s = g_s P_o (V - E_s) \tag{2.2}$$

where the probability of channel opening, P_o, is a sigmoidal function of the pressure σ_m.

$$Po = \frac{1}{(1 + k_b e^{[-s(\frac{\sigma_m}{m})^q]})} \tag{2.3}$$

To model the mechanosensory drive to the animal [30, 31], there is assumed to be a linear influx of water into the body column which gives rise to a linear increase in the

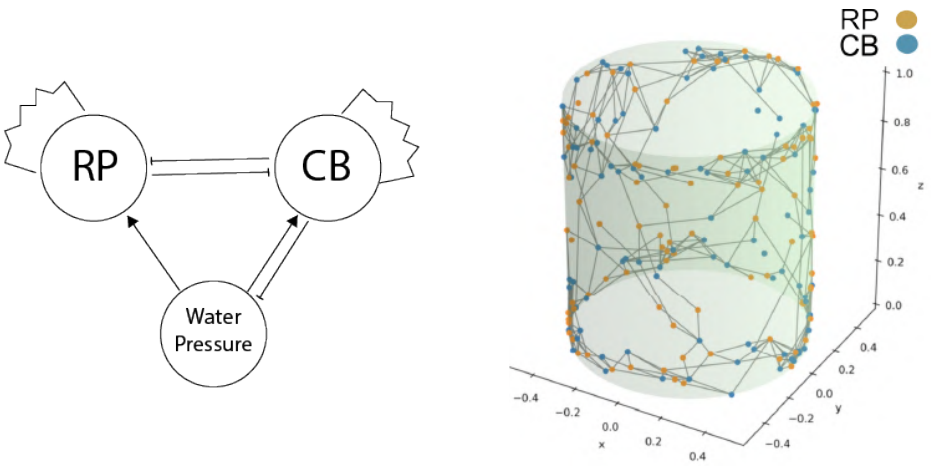

Fig. 2.1. Circuit model comprising of the RP and the CB subpopulations that are driven by the water influx and have gap junctional connections within. The RP and CB neurons are intialized on a model cylinder geometry with CB pacemakers localized near the top.

hydrostatic stress generated by water, modelled as:

$$\frac{d\sigma_w}{dt} = k_{in} - k_e \Sigma_{t^{(f)}} \delta(t - t^{(f)}). \tag{2.4}$$

Hence the water stress σ_w linearly increases with influx rate k_{in} and decreases in pulses of k_e with the firing events of the CB network, $t^{(f)}$, associated with each water expulsion due to contraction.

Activity in the contraction burst network gives rise to rapid contractions on the body column through the longitudinally oriented muscles in the ectoderm. These rapid contractions also give rise to a transient increase in active stress, σ_a, that we model as:

$$\frac{d\sigma_a}{dt} = -\frac{\sigma_a}{\tau_a} + k_a \Sigma_{t^{(f)}} \delta(t - t^{(f)}) \tag{2.5}$$

The active stress exponentially decays with time constant τ_a and increases by k_a with each firing event of the CB network, which are associated with whole body contractions.

2.2 Connectivity & spatial organization

Neurons within the same subnetwork are assumed to be gap junctionally coupled. This is based on the fact that neurons belonging to the same nerve net fire together with very little delay between pairs of neurons [10]. The gap junctions are assumed to be simple resistive channels that share current according to:

$$I^i_{gap} = g_c \Sigma_{j \in J} (V_i - V_j) \tag{2.6}$$

E_l	-75 mV
E_s	10 mV
g_l	15 nS (CB) & 1 nS (RP)
g_s	25 nS (CB pacemakers) / 2 nS (RP) / 0 nS (CB passive)
C_m	50 nF
k_a	5150 Pa
q	1
m	25
k_b	106
τ_a	5 s
λ_d	0.15 (CB inhibitory synapses) / 0.25 (RP)
I_0	40 pA
g_c	500 nS
τ_{inh}	5 s

Table 2.1: Model parameters

The activity of RP and CB networks is largely anti-correlated [6, 7, 10]. This has given rise to speculations that two networks are antagonistic and inhibit each other through chemical synapses. We model this mutual inhibition via:

$$I_{inh} = -\Sigma_{t^{(f)}} I_0 e^{-\frac{t-t^{(f)}}{\tau_{inh}}} \Theta(t - t^{(f)}) \tag{2.7}$$

Here Θ is the Heaviside step function and $t^{(f)}$ represents the firing times of the pre-synaptic neuron belonging to either the RP or CB subnetwork.

The connectivity of the neurons (for both the gap junctions within networks and the mutual inhibition synapses across networks) is distance dependent and biased longitudinally.

The CB networkis assumed to have two kinds of neurons, one with pacemaker properties that are driven by the mechanosensory drive from the water influx, and passive neurons that are driven by the pacemaker neurons through gap junctions. We assume a spatial organization of neurons with pacemaking properties based on findings from Passano & McCulloch [6, 7]. CB pacemakers are assumed to be located near the base of the hypostome, while RP pacemakers are spread throughout the body. Neurons are also packed more densely in two rings near the hypostome and the peduncle.

Both inter-network inhibitory connections and intra-network gap junctional connections were initialized randomly with a spatial exponential decay, with the probability of connection P_{ij} between two neurons, biased in the longitudinal direction, following:

$$P_{ij} \sim e^{-\frac{d_{ij}^2}{2\lambda_d^2}} \tag{2.8}$$

where the distance d_{ij} between the two neurons i and j. This is due to experimental observations that connectivity, particularly within the CB subnetwork, is more prominent longitudinally than horizontally along the body column of hydra [28]. λ_d determines the spatial scale of the decay of synaptic connectivity.

The biased distance along the cylinder is given by:

$$d_{ij} = \sqrt{(\rho(\phi_i - \phi_j)^2 + (\alpha(z_i - z_j))^2)} \tag{2.9}$$

where ϕ and z are the angle and the height coordinates of the neuron and ρ is the radius of the cylinder. The coefficient of longitudinal bias α determines how much distance along the z (height) axis is penalized, varying from 0 (being the most longitudinally biased) to 1 (least longitudinally biased). In the model simulations α was set to 0.3 for the CB network at 1 for the RP network and inter-inhibitory synapses.

2.3 Light modulation

In many of our experimental recordings of neural activity we see a trend in the neural activity of heightened firing frequency that decays from recording onset, particularly in the RP network in recordings from the regenerating peduncular half of the animal.

Previous investigations have found a positive effect of light on RP activity, along with halting of ongoing contraction bursts if the onset of light stimulus conincided with it. Using these ideas and the time scale of heightened RP frequency in our neural activity recordings I suggest the effective light driven excitation to have a decaying profile.

To model such a current I use a Hodgkin-Huxley style functional form (though any form with two time scales, one rising and one decaying, would suffice):

$$I_{light} = g_{light} m h \tag{2.10}$$

where m is the activating component and h is the inactivating component. And the activating & deactivating components following:

$$\frac{dm}{dt} = \frac{m_\infty - m_o}{\tau_m} \tag{2.11}$$

$$\frac{dh}{dt} = \frac{h_\infty - h_o}{\tau_m} \tag{2.12}$$

Based on the recordings we use the activating timescale $\tau_m = 10$ s and the deactivating timescale $\tau_h = 100$ s. Along with the gain factor $g_{light} = 40$ pA.

$$m_\infty = \frac{1}{1 + e^{-(L-0.5)}} \tag{2.13}$$

$$h_\infty = \frac{1}{1 + e^{(L-0.5)}} \tag{2.14}$$

m_∞ and h_∞ are the steady state values of the activating and the decaying component of the light current following sigmoidal relationships to the light state variable L, varying from 0 to 1, signifying on and off state of the light input.

2.4 Self-excitation in the RP network

In their analysis of neural activity preceding the somersaulting sequence, Yamamoto & Yuste found that the RP network reliably underwent a linear ramp of increasing firing frequency until it gave rise to a burst of RP activity that coincided with foot detachment in the somersault sequence [21]. In their further exploration of mechanisms underlying this, they isolate the neuropeptide Hym-248 (expressed in RP neurons) and find that its bath application can induce somersaulting along with increasing RP ramp slope and decreasing RP time, suggesting it speeds up the RP ramp. Based on this finding they suggest that the RP network self-excites itself using Hym-248.

To incorporate this self excitation and see its effect on the alternation of activity between the RP and the CB networks, I added RP to RP chemical synapses in a manner similar to the one described above with a spatially decaying probability with an excitation profile mimicking the inhibition between the networks:

$$I_{hym} = \Sigma_{t^{(f)}} I_{0_{hym}} e^{-\frac{t-t^{(f)}}{\tau_{hym}}} \Theta(t - t^{(f)}) \tag{2.15}$$

where $I_{0_{hym}}$ was set to different values between 0 to 100 pA and $t^{(f)}$ represents the firing times of the pre-synaptic RP neurons and Θ is a Heaviside function. The time scale of this self-excitation τ_{hym} was set to the same as the mutual inhibition between the two networks at 5s.

2.5 Stochastic water influx

The transitions between RP and CB activity are stochastic and this variability might underlie the expression of different behaviors, such as when, by chance, an unusually long period of elongation between two CBs might lead to enough RP excitation that it undergoes the ramp and burst needed to initiate the somersault.

In our network mechanosensitivly-driven by the osmotic pressure due to the inflow of water, this noise might arise from noise in the influx of water given the flexibility of the animal body and the vacuoles in the interstitial space that fill up with water [31]. To model this we add a noise term to the water influx equation:

$$\frac{d\sigma_w}{dt} = k_{in} - k_e \Sigma_{t^{(f)}} \delta(t - t^{(f)}) + \epsilon. \tag{2.16}$$

with ϵ is sampled from a Gaussian distribution $N(0, \sigma)$ at each time-step, where the variance $\sigma = 10{,}000$ pA.

Chapter 3

Methods

3.1 Bisection experiments

These experiments were performed by Joshua Swore in UW Biology in the laboratory of Martha Bosma [39]. The imaging setup was as described by Dupre & Yuste [10]. Whole *Hydra vulgaris* animals expressing GCaMP6s in their nerve nets were imaged for about half an hour. After this, they were bisected into a lower and upper half which were then imaged separately for half hour intervals, immediately after bisection, and then at one day intervals for the next three days. The dataset consists of these calcium videos of the freely behaving animals in the petri-dish. There are 6 animals in the dataset, and each produced 9 videos, one for the whole animal and 4 each for the oral and peduncular halves which were imaged over 4 days.

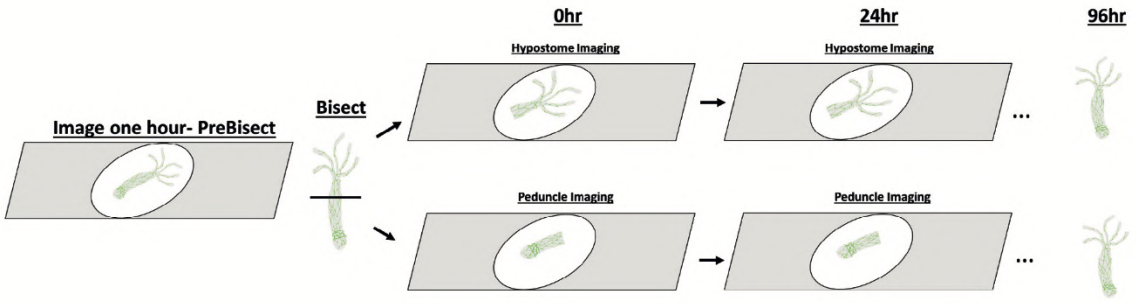

Fig. 3.1. Imaging and Bisection Protocol followed by Joshua Swore

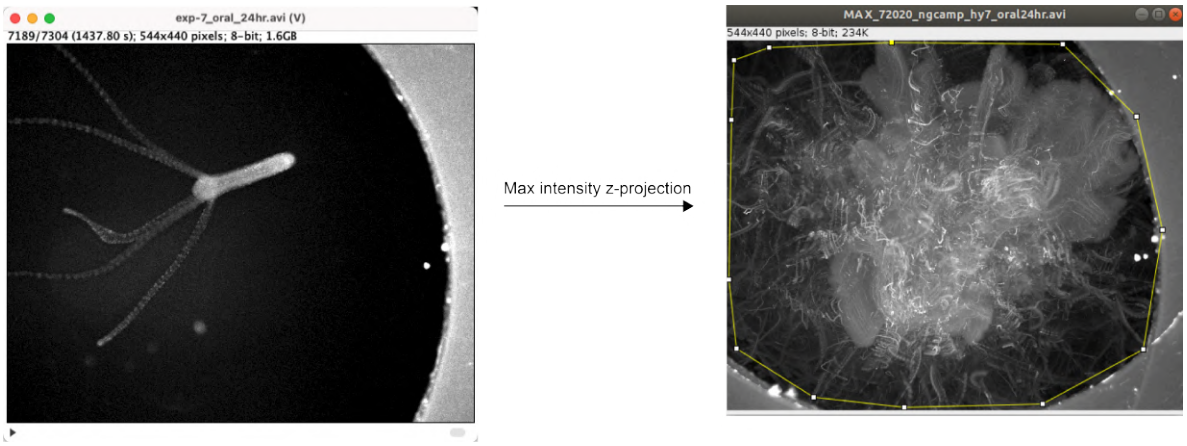

Fig. 3.2. A maximum intensity projection in time (z-axis) was used to isolate the region in the field of view where the Hydra moved to exclude transiently visible bright objects including the edge of the petri dish in the videos.

3.2 Image analysis & neural activity estimation

Z Projection and Region of Interest

Neurons are not tracked individually; rather the fluorescence signal is integrated across the body. One challenge with the data analysis is the movement of the animal. To isolate the region in the field of view of the camera in which the animal moves about the most and to exclude other objects and the petri-dish edge that appear in some videos and wash out other detail, a maximum intensity z-projection was applied on the image stack to broadly outline the region of interest. The whole body network activity was taken to be the sum of the pixel intensities in the manually determined region of interest.

Camera movement correction

Our dataset consists of videos of the freely behaving animal in a petri dish. As the animal moves about, it goes in and out of focus and often even out of the field of view of the camera. In order to keep the animal within the field of view in focus, the experimenter manually shifts the camera over the course of each imaging trial; this introduces multiple systemic errors including sudden bumps in the fluorescence trace and very bright objects coming into the field of view such as the edge of the petri dish. To fix these errors, the timepoints of camera movements were manually noted and their effect removed from the fluorescence trace.

Fluorophore decay correction

The fluorophore being used undergoes a near-linear decay over time that does not reflect a true change in the overall activity of the animal [39]. To correct for this, a linear polynomial was fit to the fluorescence time series and subtracted from it. Thie effectively straightened the decaying time series and allowed for a clearer look into

variability and peaks of neural activity.

Noise reduction

There was a lot of high frequency noise in the fluorescence time series obtained by summing light intensity in the region of interest. This noise reduces our ability to distinguish neural activity peaks, particularly for small RP network oscillations. To remove the effect of such high frequency noise, a Savitszky-Golay filter was applied to the time series, where its hyperparameters, window size and polynomial order, were manually adjusted until best resolution of neural activity could be obtained. The window-size parameter was adjusted such that it was smaller than the time course of a single RP event.

Peak finding

Using the smoothed trace, scipy's peak finding module was used to identify peaks in either the fluorescence signal itself, or its gradient, whichever yielded better identification. The hyper-parameters for peak-finding, such as prominence and peak width, were manually adjusted. After this first pass, which missed a lot of peaks, particularly for experiments with noisier time series, I went through contrast adjusted videos for each trial frame by frame and visually identified RP and CB activity and labeled them separately while using the shape of each potential peak and its gradient to corroborate it as a potential RP or CB event.

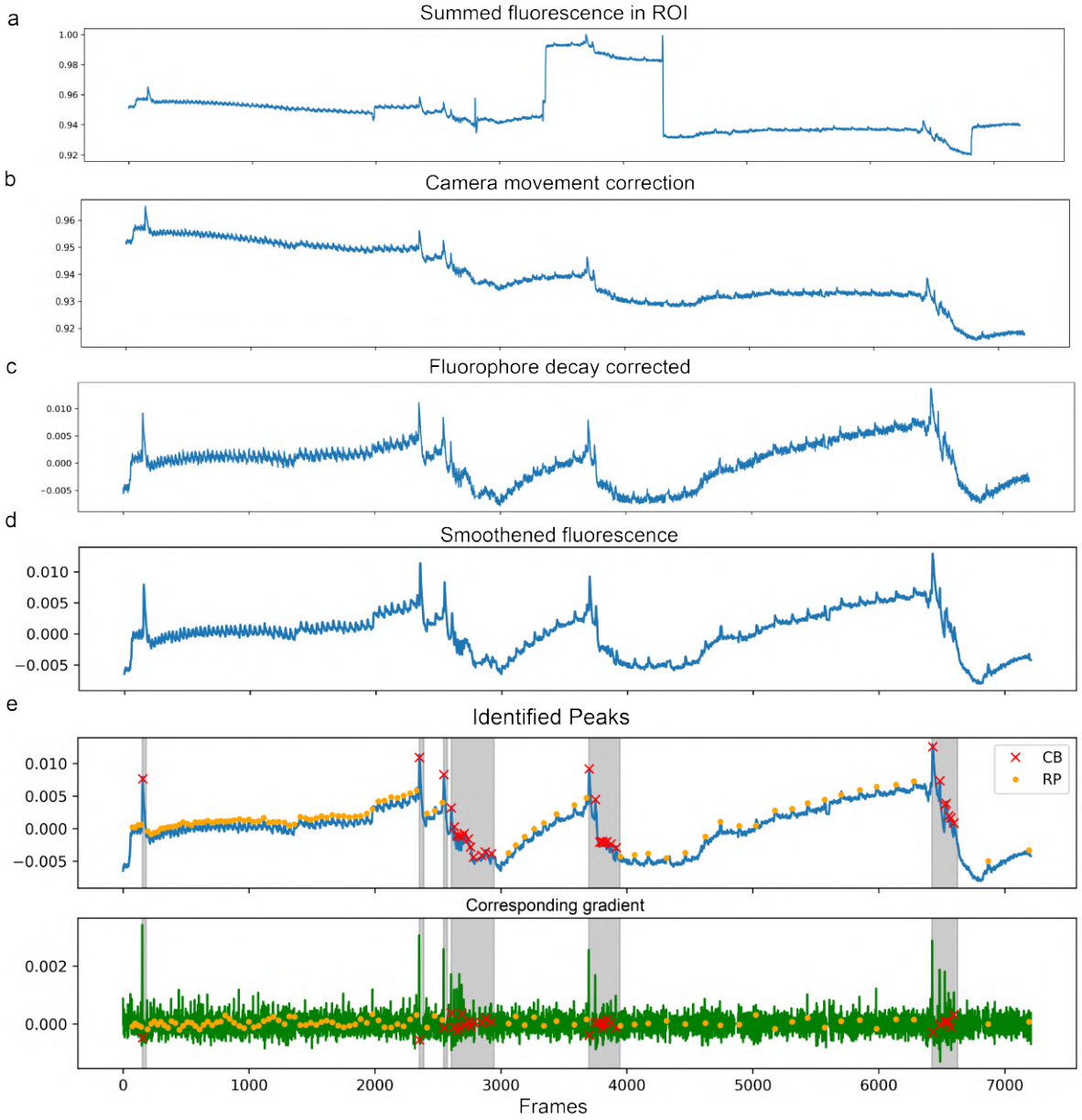

Fig. 3.3. Fluorescence processing pipeline in sequence. A. The summed fluorescence time series in the region of interest defined manually over the maximum intensity z-projection. B. Fluorescence after removing abrupt changes due to camera movement. C. Fluorescence after correcting for fluorophore decay by linear polynomial subtraction. D.

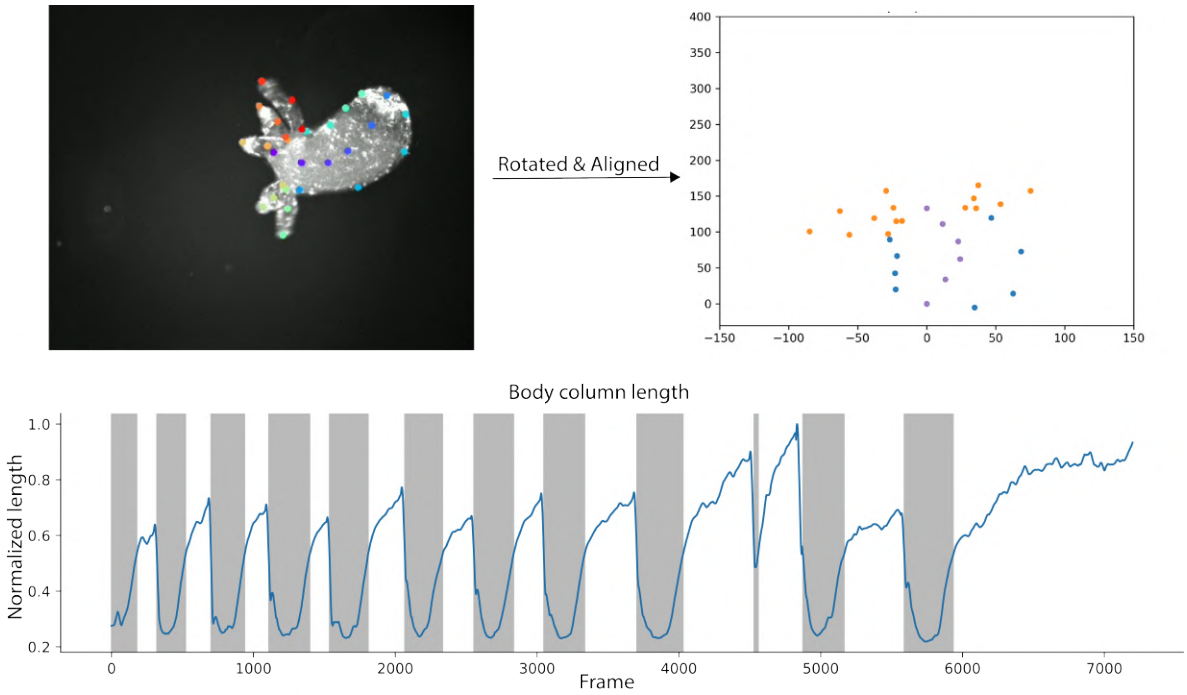

Fig. 3.4. DeepLabCut was used to label keypoints along the body to characterise the shape and length of the animal in post processing. Points were labeled along the midline, the edges and the tentacles. These were then rotated and aligned to remove translational artefacts. Length was estimated through segments along the midline and contractions estimated using a threshold.

3.3 Behavioral analysis and length extraction

The length forms one major component of the behavioral readout relevant for our study as it describes the contractile state of the animal. To extract that from the videos, keypoints were labeled along the midline of the animal's body and the sum of the segments between these points were taken as the length readout. These keypoints were labeled and tracked using the markerless pose-estimation tool DeepLabCut [24].

For a richer behavioral analysis, more points were labeled along the length of the animal and its sides along with the tentacles in videos of whole animals and the hypostomal halves. Oral halves are challenging to analyze as the animal frequently rotates to an open configuration in the plane of the imaging, so that length cannot be accurately measured.

The length was extracted from each frame as the sum of the line segments joining the midpoints labeled through deeplabcut. The time series was then smoothened using a Savitzky-Golay filter to remove high frequency jitter. After this, contraction events were determined by thresholding the length series using a manually caliberated threshold determined for each video to isolate contractions without including bends and sharp drops due to errors in tracking pose.

3.4 Statistical tests

For the significance testing of contraction burst frequency in the neural activity and the length contraction events observed via pose-estimation, I tested the data for normality using Shapiro test. The data did not pass these tests and so non-parametric tests were used subsequently. Kruskal-Wallice test was used for significance testing followed by a post-hoc Dunn's test with Bonnferroni correction.

Chapter 4

Results

The model is composed of two populations of leaky integrate and fire neurons that are gap junctionally connected within each ensemble, and that mutually inhibit each other. Neurons in both the populations are driven by a mechanosensitive current that is itself driven by linear water influx into the assumed body column.

We compare the model with recorded Hydra neural activity from a calcium imaging dataset consisting of videos of freely moving Hydra in a petri dish mounted between cover slips (see Methods). Neural activity was read out through changes in calcium fluorescence summed over the entire animal and manually spike sorted as arising from the CB or the RP sub-networks.

4.1 Whole animal model

The network activity as extracted from calcium video recordings of the whole animal of about 30 mins each is shown in (Fig 4.1). The activity alternates quasi periodically between the two sub-networks. There is some inter-animal variation and the frequency of CB bursts seems to decrease from recording onset within each trial. The model is able to capture the general pattern of alternation between the two sub-networks with a CB burst and rhythmic activity of the RP network. The raster plots of the 100 neurons in both the CB and the RP network also show the tight synchrony induced by strong gap-junctional coupling in the networks.

The firing pattern of the CB burst shows a characterising "parabolic bursting" (Fig 4.2) pattern that has also been observed in previous studies based on electrophysiology [6]. In this pattern, the inter-spike interval is shorter in the middle of the burst than at the start and the end. The underlying mechanism in the model that gives rise to bursting is the interplay of two variables, water stress and active stress; their interaction leads to parabolic bursting as is also seen in the whole animal neural recordings.

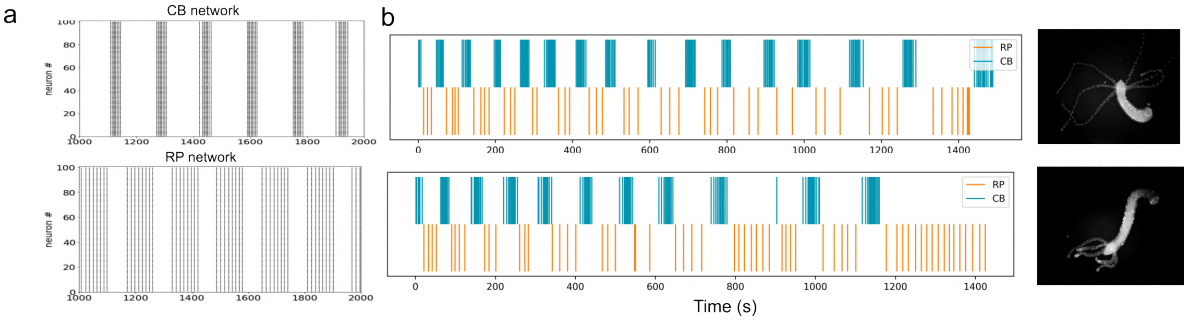

Fig. 4.1. A. Raster plots of the CB (top) and RP (bottom) sub-networks in model simulations. B. Raster plots of CB and RP neural activity observed from two whole animal preparations

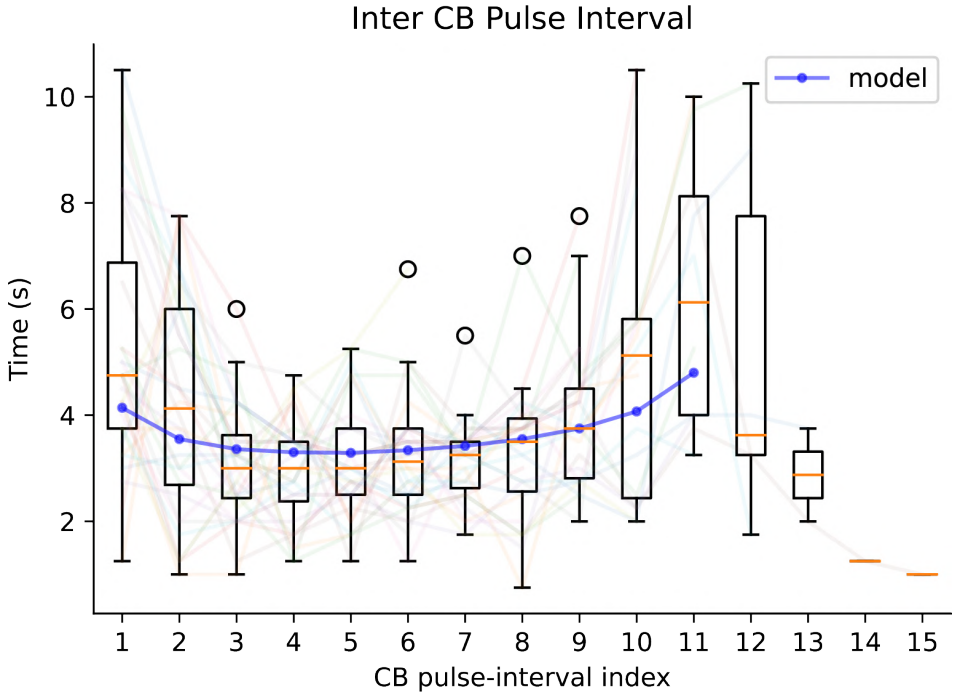

Fig. 4.2. Parabolic bursting pattern in the contraction burst (CB) events of neural activity extracted from whole animal preparations, with the model CB inter-spike-interval in blue.

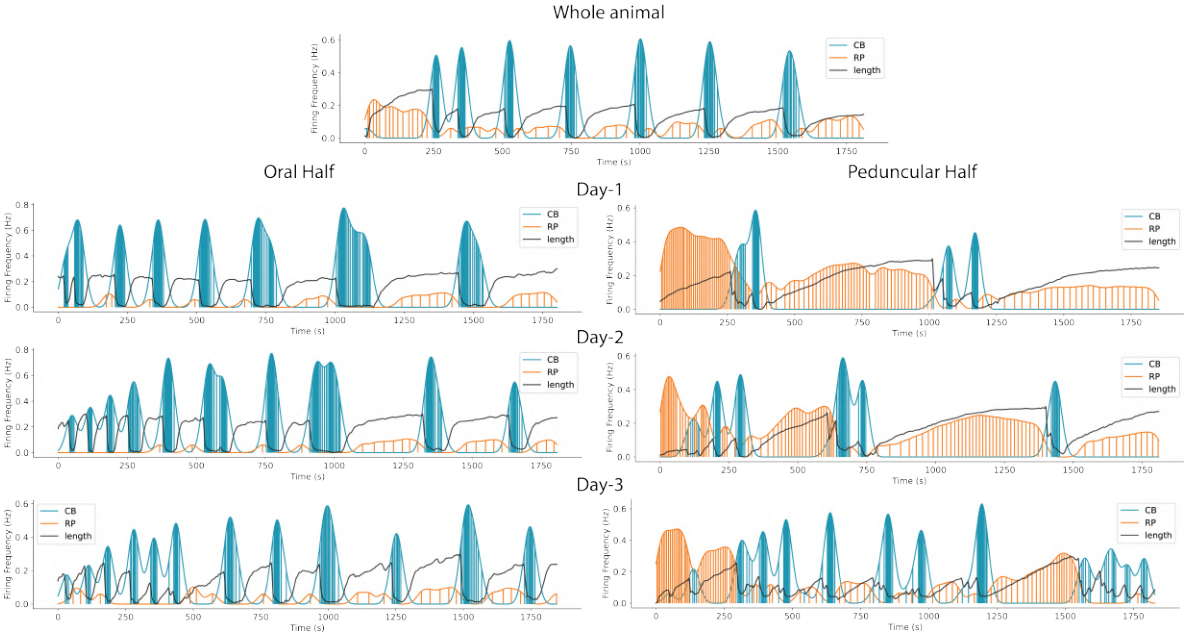

Fig. 4.3. Neural activity over the course of regeneration in a single animal along with length (black). Top. whole animal before bisection. Left column: Peduncular half recorded on days-1, 2 & 3 post-bisection. Right column: Oral half recorded over same time intervals. In each plot bars in orange represent firing events of the RP network and in blue that of the CB network, the envelope is the instantaneous rate computed with convolving a Gaussian kernel over the spiketrain. Relative body column length of the animal is superimposed, in black, without units for visual corroboration of the association between neural activity and body movements.

4.2 Regenerating halves

The network activity in the two halves showed marked differences compared to the whole animal's activity before bisection. The oral half largely preserved the frequency of contraction bursts, though higher order statistics, such as the duration of contraction burst and the number of pulses per contraction changes, and these changes are also animal specific, potentially also arises out of differences in the precise location along the length of the animal where the bisection is made (in which there is little control) and might affect to what extent the pacemaker-type neurons are removed.

The peduncular half shows very little CB activity when imaged just after bisection (Day 0), though we often see a small burst or a couple CB pulses within a few minutes of recording onset. This reduced CB frequency is likely a result of the absence of the pacemaking neurons of the CB network that are located in the hypostomal ring at the base of the tentacles. CB frequency recovers day by day as the animal regenerates, coming close to the whole animal's activity by the third day after bisection. The animal also shows more single peaks (and shorter contraction bursts) in both contraction and in the neural activity of the CB network during regenerating phases (around day 0, 1 and 2 post-bisection) in the lower half. Since the activity recovers over time gradually

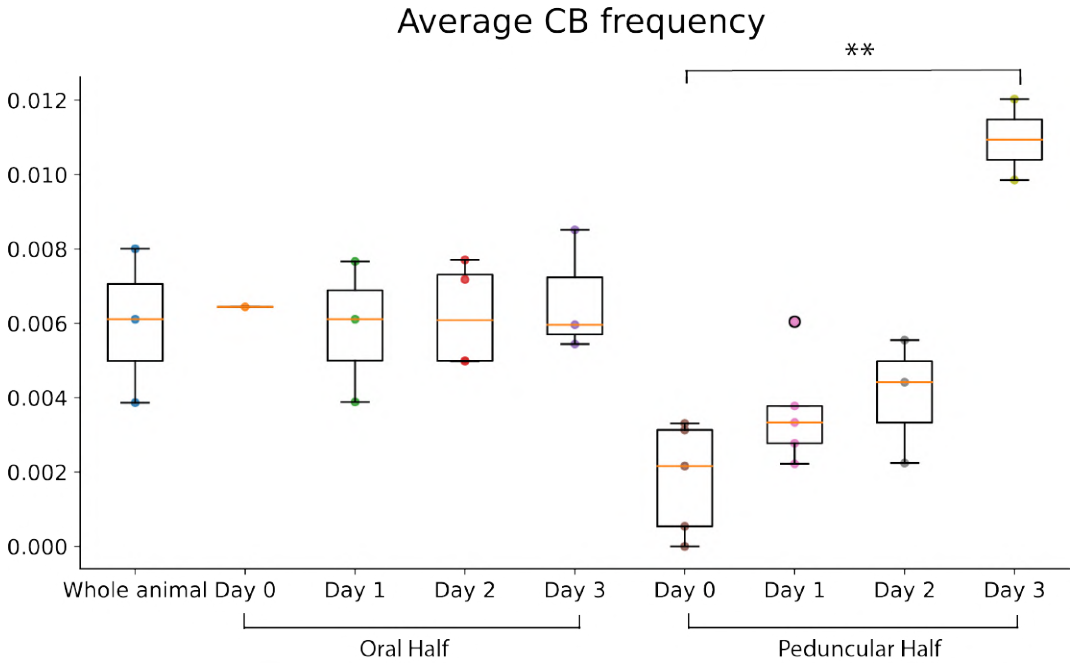

Fig. 4.4. Average Contraction Burst (CB) frequency distribution over all experimental preparations. The oral halfs don't show much deviation from the pre-bisected animal but the peduncular half effectively loses contractions and regains them over the course of regeneration. (**: p-value$<$0.01, Kruskal-Wallis followed by post-hoc Dunn's test with Bonferroni correction)

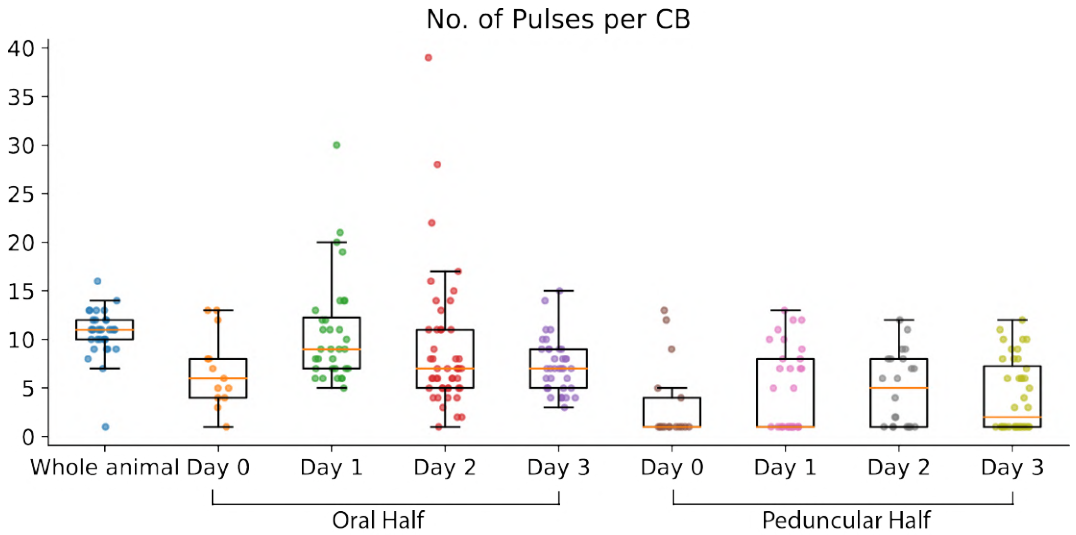

Fig. 4.5. No. of pulses per contraction burst (CB) in the pre-bisected whole animal and the two halves (oral and peduncular) over Day-0 to Day-3 of regeneration.

this suggests that there might be a gradual incorporation of pacemaker-like neurons in the CB sub-network through the growth at the oral tip in the peduncular half.

Recent investigations into the architecture of the Hydra nerve net also suggest that growth of the network occurs through the gradual incorporation of neurons [41]. These animals also start showing tentacular stubs around two to three days after bisection in line with growth near the oral tip.

Another pattern that is visible in the firing activity of the RP network in recordings from the lower half is a heightened firing frequency near the beginning of the recording. The RP frequency decays to a more steady value in about 10 mins. The frequency decreases much further if the RP activity is interrupted by a CB burst. We hypothesize that the high frequency of the rhythmic potentials in the peduncular half at the beginning of each recording interval is due to the light sensitivity of the network and the fact that our imaging setup based on GCaMP6s requires illumination. And this illumination likely occurs in the spectral range at which the network is most sensitive to light (i.e. the blue-green component of visible light) [32].

RP firing frequency also seems to be a function of delay since last CB event, i.e. the RP network fires stronger when there is a longer gap between successive CBs. The higher frequency of RP firing in longer elongation bouts fits with our hypothesis of the osmotic drive behind the firing of the network which would drive the RP network strongly if there is no release through contraction. It might also be resulting from self-excitation in the network as has been suggested recently in the context of somersaulting [21].

The recovering peduncular half also shows a high propensity for single (or isolated) contraction pulses that do not form part of a full contraction burst. Our model does not show any such single contraction events in the regenerating animal, as it relies on a osmotic drive to the CB network, with a combination of water stress (due to influx) and active stress (caused temporarily due to the contraction of the body) which always result in a burst. The presence of these single bursts indicate a potential network mechanism relying on an intrinsic pacemaking mechanism at the cellular level which might get affected due to severing of connections and give rise to single contraction events that do not cascade into a full burst.

4.3 Length and behavioral analysis

The length of the animal serves as the primary behavioral measure that is altered through its spontaneous contractions. We mark points along the midline of the animal's body from mouth to foot to approximate its length as it engages in behavior. We find that, as expected, the length contractions closely align with the neural activity of the contraction burst network. The contraction frequency obtained from the length readout matches that of the contraction burst frequency.

When the animal is bisected, the two halves behave differently. The oral half shows a mildly increased frequency of contractions while the lower half nearly stops contracting.

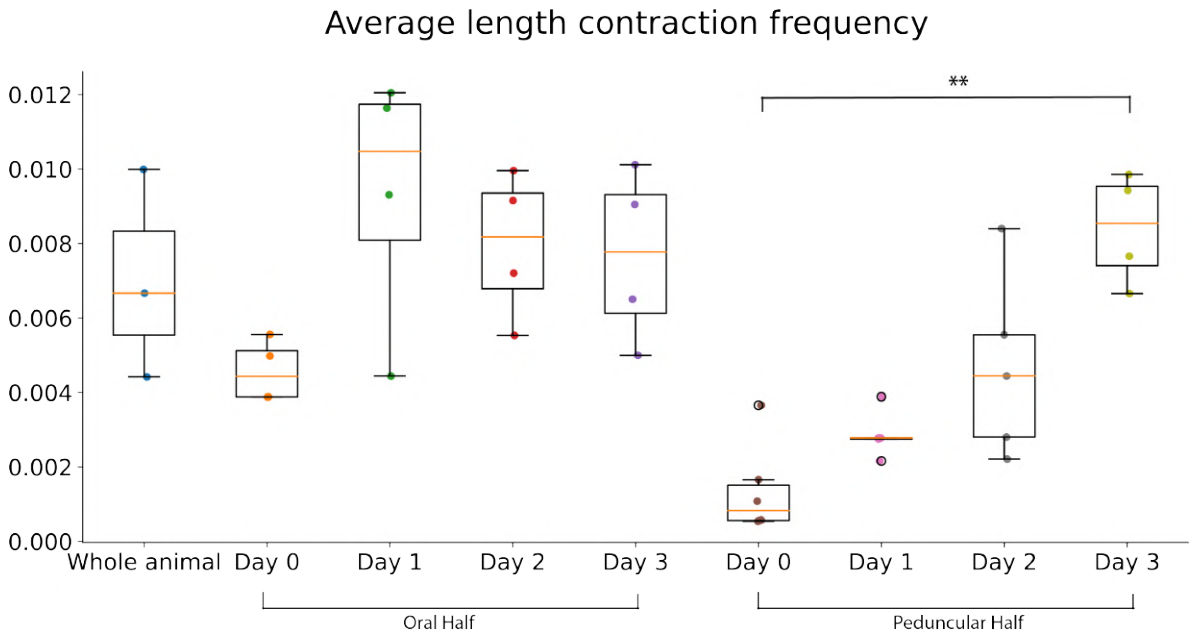

Fig. 4.6. Contraction frequency of the pre-bisected animals and the two regenerating halves over recording intervals across days 0 to 3 post-bisection, determined based on a threshold over the animal length adapted to each animal (**: p-value$<$0.01, Kruskal-Wallis followed by post-hoc Dunn's test with Bonferroni correction).

This contraction rate gradually recovers in the lower half as the animal regenerates, attaining close to normal frequencies by day three post-bisection.

The length as extracted from keypoint tracking and pose estimation tracks very closely the neural activity extracted through peak finding and manual annotation (Fig 4.6). For each single contraction neural peaks that are frequent in the regenerating lower half, there is an associated fall in length which suggests the isolation contraction events in the neural activity still activate epitheliomuscular cells responsible for contractions.

The behavioral repertoire of Hydra has been characterized with a machine learning analysis using a 'bag of words' approach to extract relevant features in an unsupervised clustering method [13] but this is a complicated method that is not easily applicable. We instead try to characterize the behavior of the animal by marking keypoints along its midline, its edges and its tentacles.

From the keypoints along the midline, which are labeled to track points of maximum curvature along the line, we interpolate the full midline of the animal and plot the bending in time by aligning the midlines to start at the origin and keeping the head constrained on the positive y-axis (Fig 4.7, see Appendix for bending dynamics in more animals). The bending dynamics of the regenerating animal show how bending recovers in the two halves . In this animal, shown in the figure, immediately after bisection the oral half loses bending, while the peducunular half only exhibts bends in one direction. Slowly the bending becomes more symmetric and increases in amplitude as the two halves regenerate.

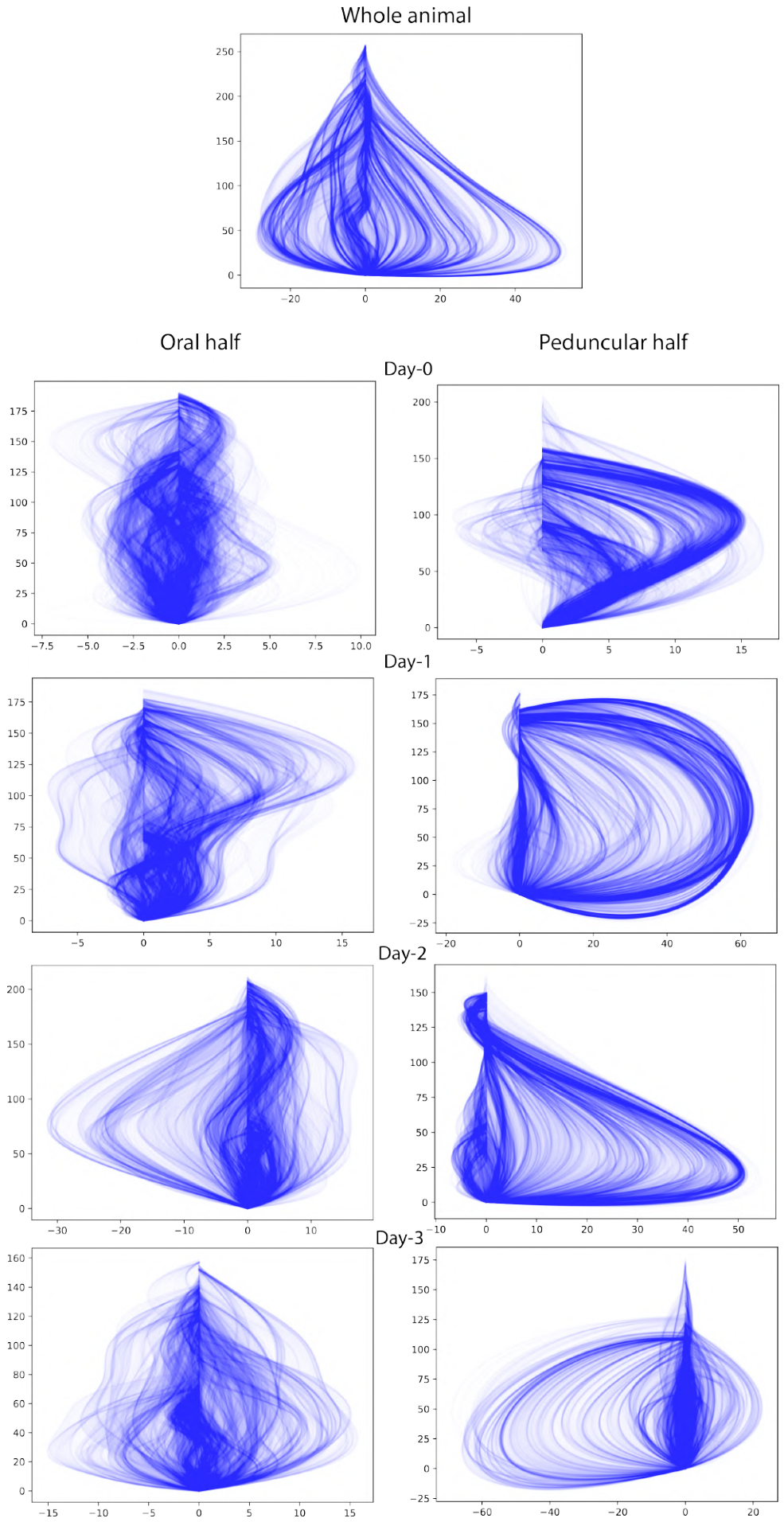

Fig. 4.7. Hydra bending dynamics superimposed over time for the prebisected animal (top) and the oral (left column) and peduncular (right column) halves as they regenerate, over day 0, 1, 2, & 3 post-bisection. In each plot, the foot of the animal is centered at (0, 0) and the body is aligned to to the +ve y-axis.

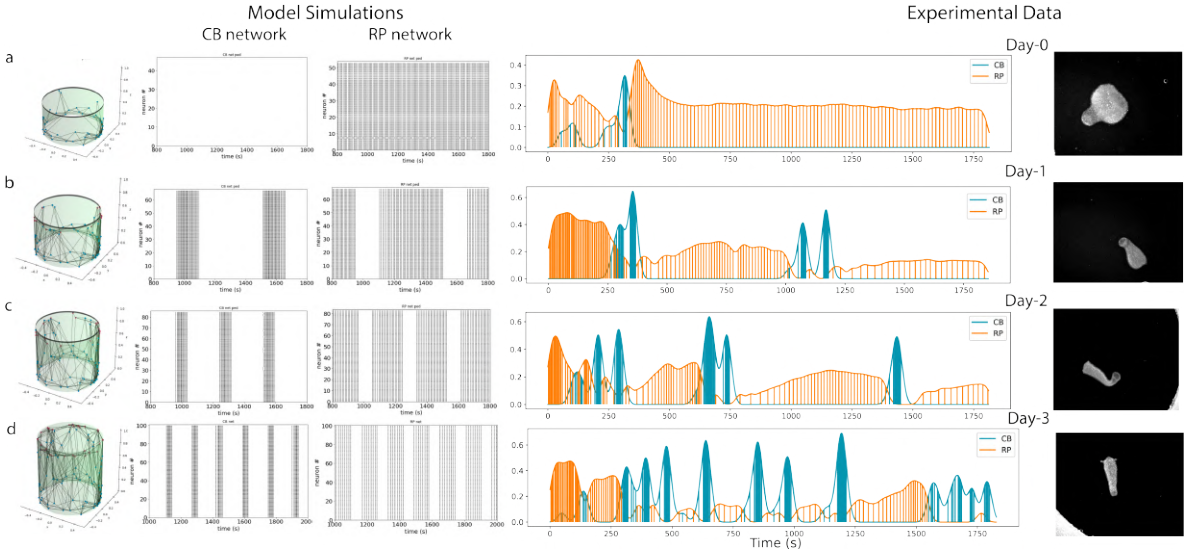

Fig. 4.8. Regeneration modeling for the lower half of the hydra body column. A. just after bisection along the midline, there are no CB pacemakers left, and the model simulation shows no CB activity. B. 1 day post-bisection, a few (15) CB pacemakers are added at the top edge of the model geometry along with more connections, this gives rise to some CB activity in the model, mirroring the increase in CB frequency in the data. C. 20 CB pacemakers added to reflect the activity of day-2 post bisection. D. All CB pacemakers added along with the connectivity of the whole animal.

4.4 Regeneration modeling

Based on recent experiments, it is known that incorporation of neurons into the functional circuit occurs gradually at the periphery of the network, where new neurons are continually added to the functioning network [41]. Using this as an assumption in our model, we study the regeneration and recovery of neural activity in the animal after being bisected. We focus on the lower half of the animal. The bisection is modeled by severing of connections along the horizontal midline of the animal.

By simulating this in our network, we see that all contractions are halted in the lower half, as a result of the removal of the CB pacemaker neurons that are located in the hypostomal ring (Fig 4.8). We do not know the rate of neurogenesis in the network, but based on the observations of CB frequency in the growing peduncular half, it is clear that CB frequency overshoots that observed in the pre-bisected whole animal.

For Day-0 of the bisection, the model has half the RP neurons and no CB pacemaker neurons. By severing connections in our model and then gradually adding CB pacemaker neurons at the top edge and proportionately adding back connections, replicating regeneration, we are able to recover CB activity in the network gradually (Fig 4.8).

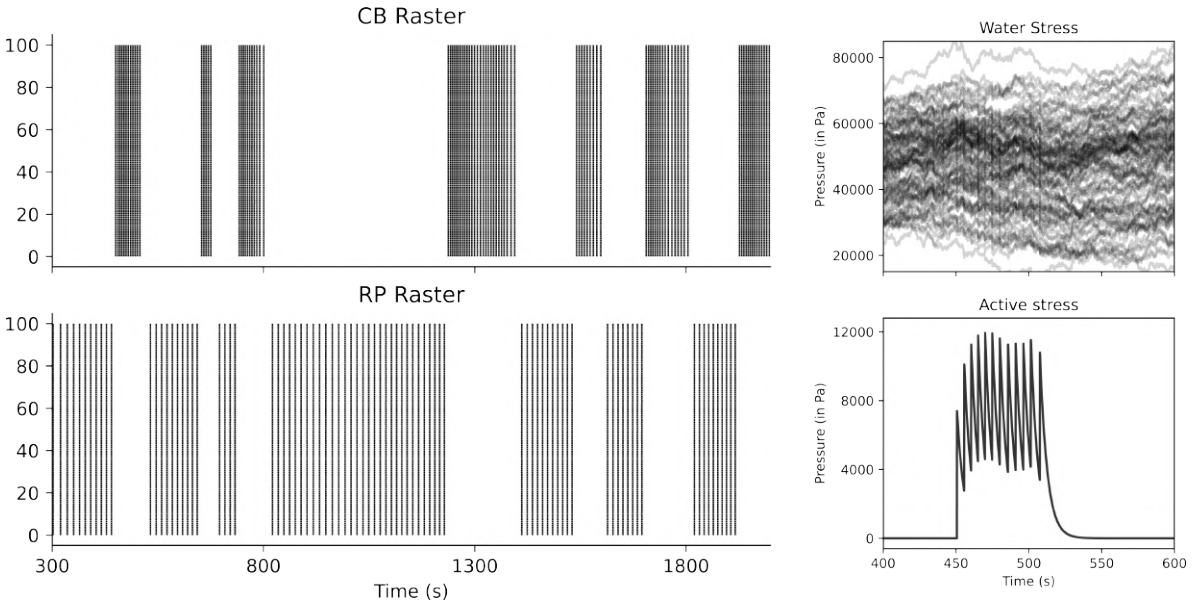

Fig. 4.9. Stochastic water influx leads to a divergence in the water stress each neuron sees (right) and the switching of activity between the CB and RP network becomes variable (left).

4.5 Stochasticity in activity switching

The switching of activity between the RP and the CB sub-networks is dynamic and shows variability depending on the size of the two networks and the regenerative state of the animal, with whole animals and regenerating animals three days after bisection showing more regular switching between the two networks than recently bisected ones.

Stochasticity in this switching can lead to the expression of different behaviors. The RP firing frequency increases the longer it takes for a successive CB burst from the last burst to occur, due to increasing osmotic drive to the network, and a ramp in RP frequency has been linked to the initiation of a somersault [21].

In our model, we assume both the RP and CB networks are primarily driven by mechanosensory currents due to the inward flux of water. This flux and the filling up of inter-cellular vacuoles in hydra is likely to be non-uniform across different components of they hydra body, given the flexible body of the animal which might drive neurons non-uniformly.

Based on this idea, we tried to incorporate noise in the water influx by driving each neuron with an independent noisy water influx. This causes changes in the periodicity of switching (Fig 4.9). We also expect such noise to be spatially correlated in the animal, thus driving clusters of neurons more strongly or more weakly and hence leading to a higher degree of stochasticity than we see here when each neuron is driven with an independent noisy water influx. On the other extreme, if all neurons are driven by a completely correlated (hence identical) noisy water influx we are able to drive a higher degree of variability in the firing of the nerve network.

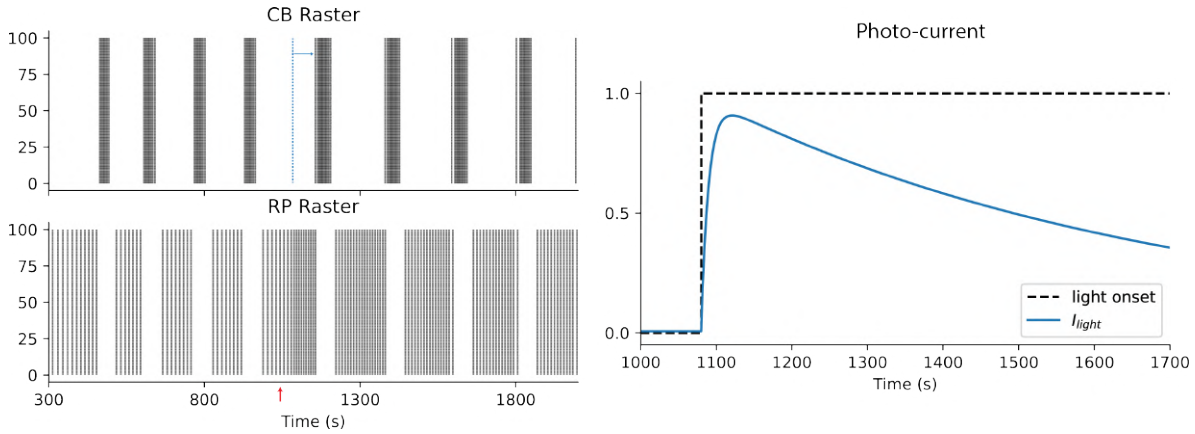

Fig. 4.10. (Left) Raster plots of the CB and the RP subnetworks with RP network driven by a light sensitive current (onset marked by red arrow). Expected CB burst time indicated by dashed blue line. The delay of the succeeding CB burst is illustraed with blue arrow. (Right) The profile of the photocurrent (in blue) applied uniformly to the RP network with light onset (dashed black line).

4.6 Light modulation

In the neural activity extracted from the bisection experiments we see a heightened RP firing frequency at the beginning of each trial in the case of the regenerating lower half. We assume that this is an experimental artifact arising due to the nature of the calcium imaging setup which involves excitation of the GCaMP fluorophore with blue-green light, which is close to wavelength that maximally excites hydra neural activity as seen in previous electrophysiological studies [6, 7, 32].

Using these ideas and the neural recordings from the bisection dataset we speculate on the nature of light driven excitation of the RP circuit by driving it with a current taking the shape in Fig 4.10. This is based on the profile of excitation of the RP network observed in the regenerating lower half at the beginning of each recording trial.

We find that this RP excitation delays the succeeding CB burst from when it would be expected to occur based on CB frequency. We also see that the succeeding CB burst, after the delay due to the light stimulus occurs with a higher intensity (i.e. has a greater number of pulses than usual). This fits with our picture of the mechanosensory drive as the basis of contractions and mutual inhibition between the RP and CB networks, as excitation of the RP network leads to a stronger inhibition of the CB network which delays the CB burst, but leads to a greater buildup of water stress in the body column resulting in a stronger CB burst. The time delay between successive CB bursts persists and decays as the photosensitive inward current to the RP network decays.

Chapter 5

Discussion

Our network model of *Hydra* combines a spatial organisation of two populations of neurons on a model cylindrical geometry with mutual inhibition between the two subnetworks, intra-network gap junctions, inter-network mutual inhibition and a mechanosensory drive due to water influx as the primary driver of neural activity to explain the alternation between observed RP and CB activity in the animal. By doing so it provides a mechanistic understanding of how these elements come together to shape the spontaneous contractions in *Hydra*. Using a calcium imaging dataset of whole and bisected halves of the animal I validate the model and suggest expansions to make sense of the higher order variation we see in the neural activity. The model captures the inter-spike interval profile observed within contraction bursts along with the gradual recovery of contraction bursts after bisection.

The nerve net in hydra recovers gradually after the animal is bisected in two along the midline [4]. In the model of the regenerating lower half, we assume this recovery occurs via addition of the CB pacemaker neurons near the growing top along with a random growth of connections between the new neurons and the existing ones. This gradual addition of CB pacemaker qualitatively captures the recovery of the CB frequency (Fig 4.8). A recent study of the architecture of the nerve net of *Hydra* and its growth and differentiation found that gradual incorporation of neurons continually occurs at the periphery of the functioning network in a normal animal over a daily timescale [41]. Similar experiments over regeneration could provide conclusive proof of growth validating our assumptions of recovery of neural circuitry and activity.

The power of hydra as a model organism to study whole body neural activity and behavior lies in its small size and body transparency and recent amenability to transgenics. But since the animal has a flexible body (as opposed to being rigid) it has hitherto escaped precise biophysical characterization of neural properties at the cellular level via standard methods like the voltage patch-clamp. Calcium imaging and the subsequent extraction of neural activity from hydra poses a considerable challenge. The animal, when free to move, in the petri-dish moves in all directions including along the z-axis, perpendicular to the plane of the camera. This is more so in the case of the regenerating

oral half, which does not posses the peduncular basal disc to attach itself and at the same time shows a high frequency of contractions, moving about in the petri-dish and making focused calcium activity extraction more difficult. Due to this difficulty of imaging we are only able to track full body fluorescence and not single cellular level neural activity. The length tracked from our dataset via pose–estimation closely tracks the contraction burst network pulses observed via our spike detection mechanisms (Fig 4.3, also see Appendix), which corroborates our neural activity extraction method. Higher resolution calcium imaging with individual cell tracking for neural activity extraction would enhance our understanding of sub-network dynamics in the animal's body and allow incorporating smaller neural ensembles such as the sub-tentacular network into our modeling framework.

The switching of activity between the CB and the RP potentially underlies the expression of different behaviors in the animal, as in the case of somersaulting in which Yamamoto & Yuste have shown recently that the behavior is initiated when the RP network undergoes a linear ramp of increasing activity for a long duration by suppressing the CB [21]. Switching between the networks in our model relies on the osmotic drive to the two networks which have different conductances of the Peizo channel (see Methods). There are many underlying sources of noise that might underlie stochastic switching. The regenerating halves show a greater degree of variability in switching than the pre-bisected whole animal over the course of the recording intervals in our dataset (see Appendix). I found that unreliable transmission was insufficient to give rise to stochastic switching due to the tight gap junctional coupling which effectively renders the two population network into two functional units where noise due to unreliable transmission gets averaged out. When we drive the neurons in our model with a variable mechanosensory drive, assuming a non-uniform local water stress around each neuron, switching becomes stochastic. A finer biophysical characterisation of stress in the body column along with neural dynamics could better test our assumption.

The regenerating lower half shows the presence of single isolated pulses in the CB network which occur along with dips in the animal length observed from pose estimation. Our model relying on the mechanosensory drive and the interplay of active and water stress does not show isolated single contraction events. These events suggest an underlying network mechanism intrinsic to the nerve net and its pacemaking components. A more complete description underlying oscillatory activity in the hydra nerve net might need to invoke a combination of an external drive with intrinsic osciallatory mechanisms at the cellular or network level.

The whole and the regenerating animal shows interesting bending dynamics with modes in the posture space that suggest that there are preferred bends which in turn suggests that the underlying neural circuitry giving rise to the bends might have some structure to it. There has been interesting work in *C. elegans* in characterizing the eigen-decomposition of its bending dynamics as it engages in locomotion [42]. A similar analysis of stereotyped trajectories in behavioral space might

We also see higher order variation in the neural activity of the animal that the model

with its uniform alternation between the two subnetworks does not capture. Some of this variation in the activity potentially arises out of the experimental artefact of light stimulation due to imaging and the mechanical agitation caused to hydra. There has been recent behavioral characterization of the light driven somersaulting in hydra dependent on the hunger state of the animal [22]. A more detailed biophysical characterisation of hydra's response to light and other stimuli would help constrain our ideas about photo-sensitivity of the nerve net. It would be insightful to include these sensory effects into the model and study how they shape neural activity and behavior in the animal.

5.1 Future directions

Our understanding of hydra neurophysiology is still growing and the pace of new discoveries has increased due to genomic advances and better imaging methods. There is also an increased recognition of the complexity of simpler nervous systems that arises out of complexity at the cellular level and differences in the responses of neural circuits under different extracellular conditions such as can be modulated by neuropeptides.

5.1.1 Neuropeptides

Chemical interactions between the nerve nets, between neurons and epitheliomuscular cells and quite possibly within the nerve nets itself are mediated through neuropeptides [43], with multiple neuropeptides involved in the same interactions. It has been suggested the the RFamide peptide hym-248 is both necessary and sufficient to induce somersaulting the in hydra [21]. It would be very intersting to incorporate the effect of different neuropeptides in the mutual-inhibition based network model between RP & CB.

5.1.2 Tentacles

Tentacles form a significant component of the body of the hydra and are involved in its most prominent composite behaviors i.e. feeding and somersaulting. The set of neurons in the ectoderm of tentacles form one of the non-overlapping nerve nets of hydra. Though there don't seem to be neurons in the endoderm at the tentacles. While feeding, the tentacles latch onto a prey and discharge their cnidocytes which are specialized stinging cells organized radially along the tentacles in a battery cell complex. Tentacle pulses also seem to occur preceding a burst for which there isn't a clear explanation.

There is also significant evidence that much of the light sensitive response of hydra is mediated by opsins expressed in the tentacles and the head. A recent experiment suggested that the light sensitivity of the tentacles is important for the animal to discharge its cnidocytes to attack and paralyse prey [44].

It would add insight to explore how the tentacular subnetwork interacts with the CB and

the RP nerve nets, how it is affected by the state of the animal and how it coordinates the control of tentacles, particularly in the context of feeding and somersaulting.

5.1.3 Endodermal Network

The hydra nerve net possesses at least two independent nerve nets i.e. these networks do not directly interact through synapses. It is possible, however, that there might be indirect communication between the networks such as through gap junctions between the ectodermal and the endodermal muscle groups. Further, the networks may interact indirectly via feedback from mechanoreceptors responding to the animal's movement state.

The endodermal network likely plays a role in regulating the contraction of the radially oriented muscles in the gastroderm. Our model doesn't account for the activity of the endodermal network. Experimental insight into the nature of the activity of the endodermal nerve net is also scant. This provides a potential future avenue for both experimental and theoretical work on how the endodermal neural activity relates to the behavior of the animal, how it modulates the ectodermal network's activity and how they together pattern the contraction of the two muscle groups to effectively carry out contraction and somersaulting.

5.1.4 Connectivity

Our model assumes random connectivity between neurons within the same subnetwork via gap junctions and chemical synapses between the RP and the CB subnetworks. Based on previous work in other random networks, we assume exponential decay in this connectivity over a spatial constant along the body surface of the animal [45]. This assumption might not entirely hold. With recent work investigating the connectivity more insight into the morphology and subcellular structure of the nerve net has emerged that might be levaraged to incorporate more fine grained detail into the circuit connectivity that might model the hydra nerve net more closely.

5.1.5 Microbiome

In a fascinating recent line of research, Hydra has been shown to possess a rich microbiome at both the gastrointestinal and outer body wall surfaces [46]. There are significant interactions between the nervous system of hydra [47] and its microbiota to the extent that the presence of microbes directly shapes its behavior. The depletion of Hydra microbiota disrupts the eating behavior of the animal by decreasing mouth opening duration, and can be restored by adding the microbes back [48].

Depriving the Hydra of its microbiota leads to a reduction in the contraction frequency [49]. It has been argued that the purpose of spontaneous body wall contractions is to shed a fluid boundary layer that forms around a stationary animal and by this shedding allow for the microbiome to feed on a new fluid layer [50]. It would be interesting to

see how this perspective may be integrated with the proposed osmotic basis of the spontaneous contractions we investigate here.

5.1.6 Hunger & internal states

Hydra behavior is affected by its hunger state. It somersaults more often when starved [22]. Many of the experiments involving hydra have been done with animals that have been starved for a few days before being experimented upon. How the hunger state of the animal affects and interacts with the neural activity is unclear. Hunger might be tracked at the molecular level, and alter the neuropeptidergic constitution of the animal, which might affect the overall activity of the RP network, as its heightened activity is associated with the somersault. More experiments in this domain could shed light on this.

Bibliography

1. Bosch, T. C. *et al.* Back to the Basics - Cnidarians Start to Fire. *Trends in Neurosciences* **40,** 92–105. ISSN: 01662236. https://linkinghub.elsevier.com/retrieve/pii/S0166223616301680 (2022) (Feb. 2017).
2. Watanabe, H., Fujisawa, T. & Holstein, T. W. Cnidarians and the evolutionary origin of the nervous system. *Development, Growth & Differentiation* **51.** _eprint: https://onlinelibrary.wiley.com/doi/pdf/10.1111/j.1440-169X.2009.01103.x, 167–183. ISSN: 1440-169X. https://onlinelibrary.wiley.com/doi/abs/10.1111/j.1440-169X.2009.01103.x (2022) (2009).
3. Technau, U. & Steele, R. E. Evolutionary crossroads in developmental biology: Cnidaria. *Development* **138,** 1447–1458. ISSN: 0950-1991. https://doi.org/10.1242/dev.048959 (2022) (Apr. 15, 2011).
4. Lovas, J. R. & Yuste, R. Ensemble synchronization in the reassembly of Hydra's nervous system. *Current Biology* **31,** 3784–3796.e3. ISSN: 09609822. https://linkinghub.elsevier.com/retrieve/pii/S0960982221008769 (2022) (Sept. 2021).
5. Passano, L. M. & Mccullough, C. B. Pacemaker Hierarchies Controlling the Behaviour of Hydras. *Nature* **199.** Number: 4899 Publisher: Nature Publishing Group, 1174–1175. ISSN: 1476-4687. https://www.nature.com/articles/1991174a0 (2022) (Sept. 1963).
6. Passano, L. M. & McCullough, C. B. Co-Ordinating Systems and Behaviour In Hydra: I. Pacemaker System of the Periodic Contractions. *Journal of Experimental Biology* **41,** 643–664. ISSN: 0022-0949. https://doi.org/10.1242/jeb.41.3.643 (2022) (Sept. 1, 1964).
7. Passano, L. M. & McCullough, C. B. Co-Ordinating Systems and Behaviour in Hydra II. The Rhythmic Potential System. *Journal of Experimental Biology* **42,** 205–231. ISSN: 0022-0949. https://doi.org/10.1242/jeb.42.2.205 (2022) (Apr. 1, 1965).
8. Chapman, J. A. *et al.* The dynamic genome of Hydra. *Nature* **464.** Number: 7288 Publisher: Nature Publishing Group, 592–596. ISSN: 1476-4687. https://www.nature.com/articles/nature08830 (2023) (Mar. 2010).
9. Siebert, S. *et al.* Stem cell differentiation trajectories in Hydra resolved at single-cell resolution. *Science* **365.** Publisher: American Association for the Advancement of Science, eaav9314. https://www.science.org/doi/10.1126/science.aav9314 (2023) (July 26, 2019).

10. Dupre, C. & Yuste, R. Non-overlapping Neural Networks in Hydra vulgaris. *Current Biology* **27,** 1085–1097. ISSN: 09609822. https://linkinghub.elsevier.com/retrieve/pii/S0960982217302208 (2022) (Apr. 2017).
11. Yamamoto, W. & Yuste, R. Whole-Body Imaging of Neural and Muscle Activity during Behavior in Hydra vulgaris: Effect of Osmolarity on Contraction Bursts. *eNeuro* **7.** Publisher: Society for Neuroscience Section: Research Article: Methods/New Tools. ISSN: 2373-2822. https://www.eneuro.org/content/7/4/ENEURO.0539-19.2020 (2022) (July 1, 2020).
12. Gooshvar, S., Madhu, G., Ruszczyk, M. & Prakash, V. N. *Non-bilaterians as Model Systems for Tissue Mechanics* June 2, 2023. arXiv: 2306.01935[physics,q-bio]. http://arxiv.org/abs/2306.01935 (2023).
13. Han, S., Taralova, E., Dupre, C. & Yuste, R. Comprehensive machine learning analysis of Hydra behavior reveals a stable basal behavioral repertoire. *eLife* **7** (ed Calabrese, R. L.) Publisher: eLife Sciences Publications, Ltd, e32605. ISSN: 2050-084X. https://doi.org/10.7554/eLife.32605 (2023) (Mar. 28, 2018).
14. Kanaya, H. J. *et al.* A sleep-like state in Hydra unravels conserved sleep mechanisms during the evolutionary development of the central nervous system. *Science Advances* **6.** Publisher: American Association for the Advancement of Science, eabb9415. https://www.science.org/doi/10.1126/sciadv.abb9415 (2022) (Oct. 7, 2020).
15. Wilson, E. B. The Heliotropism of Hydra. *The American Naturalist* **25.** Publisher: The University of Chicago Press, 413–433. ISSN: 0003-0147. https://www.journals.uchicago.edu/doi/10.1086/275328 (2024) (May 1891).
16. Carter, J. A., Hyland, C., Steele, R. E. & Collins, E.-M. S. Dynamics of Mouth Opening in *Hydra*. *Biophysical Journal* **110,** 1191–1201. ISSN: 0006-3495. https://www.sciencedirect.com/science/article/pii/S0006349516000527 (2024) (Mar. 8, 2016).
17. Rushforth, N. B., Burnett, A. L. & Maynard, R. Behavior in Hydra: Contraction Responses of Hydra pirardi to Mechanical and Light Stimuli. *Science* **139.** Publisher: American Association for the Advancement of Science, 760–761. https://www.science.org/doi/10.1126/science.139.3556.760 (2022) (Feb. 22, 1963).
18. Wang, H. *et al. From neuron to muscle to movement: a complete biomechanical model of Hydra contractile behaviors* Section: New Results Type: article (bioRxiv, Dec. 15, 2020), 2020.12.14.422784. https://www.biorxiv.org/content/10.1101/2020.12.14.422784v1 (2022).
19. Koizumi, O., Haraguchi, Y. & Ohuchida, A. Reaction chain in feeding behavior ofHydra: Different specificities of three feeding responses. *Journal of comparative physiology* **150,** 99–105. ISSN: 1432-1351. https://doi.org/10.1007/BF00605293 (2024) (Mar. 1, 1983).
20. Lenhoff, H. M. Activation of the Feeding Reflex in Hydra littoralis : I. Role played by reduced glutathione, and quantitative assay of the feeding reflex. *Journal of General Physiology* **45,** 331–344. ISSN: 0022-1295. https://doi.org/10.1085/jgp.45.2.331 (2024) (Nov. 1, 1961).

21. Yamamoto, W. & Yuste, R. Peptide-driven control of somersaulting in Hydra vulgaris. *Current Biology* **33,** 1893–1905.e4. ISSN: 09609822. https://linkinghub.elsevier.com/retrieve/pii/S0960982223003354 (2023) (May 2023).
22. Kim, S. & Robinson, J. T. *Phototaxis is a state-dependent behavioral sequence in Hydra vulgaris* preprint (Systems Biology, May 13, 2023). http://biorxiv.org/lookup/doi/10.1101/2023.05.12.540432 (2023).
23. McCullough, M. H. & Goodhill, G. J. Unsupervised quantification of naturalistic animal behaviors for gaining insight into the brain. *Current Opinion in Neurobiology. Computational Neuroscience* **70,** 89–100. ISSN: 0959-4388. https://www.sciencedirect.com/science/article/pii/S0959438821000891 (2024) (Oct. 1, 2021).
24. Nath, T. *et al.* Using DeepLabCut for 3D markerless pose estimation across species and behaviors. *Nature Protocols* **14.** Number: 7 Publisher: Nature Publishing Group, 2152–2176. ISSN: 1750-2799. https://www.nature.com/articles/s41596-019-0176-0 (2022) (July 2019).
25. Berman, G. J., Choi, D. M., Bialek, W. & Shaevitz, J. W. Mapping the stereotyped behaviour of freely moving fruit flies. *Journal of The Royal Society Interface* **11.** Publisher: Royal Society, 20140672. https://royalsocietypublishing.org/doi/10.1098/rsif.2014.0672 (2024) (Oct. 6, 2014).
26. Westfall, J. A., Kinnamon, J. C. & Sims, D. E. Neuro-epitheliomuscular cell and neuro-neuronal gap junctions inHydra. *Journal of Neurocytology* **9,** 725–732. ISSN: 1573-7381. https://doi.org/10.1007/BF01205015 (2024) (Dec. 1, 1980).
27. Takaku, Y. *et al.* Innexin gap junctions in nerve cells coordinate spontaneous contractile behavior in Hydra polyps. *Scientific Reports* **4.** Publisher: Nature Publishing Group, 3573. ISSN: 2045-2322. https://www.nature.com/articles/srep03573 (2024) (Jan. 7, 2014).
28. Kass-Simon, G. Longitudinal conduction of contraction burst pulses from hypostomal excitation loci inHydra attenuata. *Journal of comparative physiology* **80,** 29–49. ISSN: 1432-1351. https://doi.org/10.1007/BF00694326 (2022) (Mar. 1, 1972).
29. Hanson, A. On being a Hydra with, and without, a nervous system: what do neurons add? *Animal Cognition.* ISSN: 1435-9456. https://doi.org/10.1007/s10071-023-01816-8 (2023) (Aug. 4, 2023).
30. Benos, D. J. & Prusch, R. D. Osmoregulation in fresh-waterHydra. *Comparative Biochemistry and Physiology Part A: Physiology* **43,** 165–171. ISSN: 0300-9629. https://www.sciencedirect.com/science/article/pii/0300962972904781 (2024) (Sept. 1, 1972).
31. Benos, D. J., Kirk, R. G., Barba, W. P. & Goldner, M. M. Hyposmotic fluid formation in Hydra. *Tissue and Cell* **9,** 11–22. ISSN: 0040-8166. https://www.sciencedirect.com/science/article/pii/0040816677900453 (2024) (Jan. 1, 1977).
32. Taddei-Ferretti, C. & Musio, C. Photobehaviour of Hydra (Cnidaria, Hydrozoa) and correlated mechanisms: a case of extraocular photosensitivity. *Journal of Photochemistry and Photobiology B: Biology* **55,** 88–101. ISSN: 1011-1344. https:

//www.sciencedirect.com/science/article/pii/S1011134400000415 (2023) (May 30, 2000).
33. Taddei-Ferretti, C. & Cordella, L. Modulation of Hydra attenuata rhythmic activity: phase response curve. *Journal of Experimental Biology* **65,** 737–751. ISSN: 0022-0949. https://doi.org/10.1242/jeb.65.3.737 (2022) (Dec. 1, 1976).
34. Taddei-Ferretti, C. & Chillemi, S. Modulation of Hydra Attentuata rhythmic activity. *Biological Cybernetics* **56,** 225–235. ISSN: 1432-0770. https://doi.org/10.1007/BF00365217 (2022) (June 1, 1987).
35. Taddei-Ferretti, C., Musio, C., Santillo, S. & Cotugno, A. The photobiology of Hydra's periodic activity. *Hydrobiologia* (2004).
36. Birch, S. & Link to external site, t. l. w. o. i. a. n. t. *Integrating Behavior and Genomics to Understand Sensory Integration in Cnidarians* ISBN: 9798819397596. PhD thesis (University of New Hampshire, United States – New Hampshire, 2022). 223 pp. https://www.proquest.com/docview/2682274419/abstract/93AD79F53F594F12PQ/1 (2023).
37. Guertin, S. & Kass-Simon, G. Extraocular spectral photosensitivity in the tentacles of Hydra vulgaris. *Comparative Biochemistry and Physiology Part A: Molecular & Integrative Physiology* **184,** 163–170. ISSN: 1095-6433. https://www.sciencedirect.com/science/article/pii/S1095643315000380 (2023) (June 1, 2015).
38. Guertin, S. L. *A genomic and electrophysiological study of photoreception in the eyeless cnidarian Hydra vulgaris* ISBN: 9781303886591. PhD thesis (University of Rhode Island, United States – Rhode Island, 2015). 129 pp. https://www.proquest.com/docview/1537075732/abstract/8AE9EE0ECC6C4B04PQ/1 (2023).
39. Swore, J. J. *Molecular and Biophysiological Differences in Neuronal Innexin Gap Junctions Likely Underlie Unique Circuit Behaviors in Hydra vulgaris* ISBN: 9798426801615. PhD thesis (University of Washington, United States – Washington, 2022). 158 pp. https://www.proquest.com/docview/2652017561/abstract/7561D89D419942F0PQ/1 (2022).
40. Wang, H. *Modeling Hydra from neuron to muscle to behavior* PhD thesis (University of Washington, 2022). https://digital.lib.washington.edu/researchworks/handle/1773/49430.
41. Keramidioti, A. *et al.* A new look at the architecture and dynamics of the Hydra nerve net. *eLife* **12** (ed Desplan, C.) Publisher: eLife Sciences Publications, Ltd, RP87330. ISSN: 2050-084X. https://doi.org/10.7554/eLife.87330 (2024) (Feb. 26, 2024).
42. Stephens, G. J., Johnson-Kerner, B., Bialek, W. & Ryu, W. S. Dimensionality and Dynamics in the Behavior of C. elegans. *PLOS Computational Biology* **4.** Publisher: Public Library of Science, e1000028. ISSN: 1553-7358. https://journals.plos.org/ploscompbiol/article?id=10.1371/journal.pcbi.1000028 (2024) (Apr. 25, 2008).
43. Takahashi, T., Hayakawa, E., Koizumi, O. & Fujisawa, T. Neuropeptides and their functions in Hydra. *Acta Biologica Hungarica* **59.** Publisher: Akadémiai Kiadó Section: Acta Biologica Hungarica, 227–235. ISSN: 0236-5383, 1588-256X. https:

//akjournals.com/view/journals/018/59/10002/article-p227.xml (2023) (Issue Supplement-2 June 3, 2008).
44. Plachetzki, D. C., Fong, C. R. & Oakley, T. H. Cnidocyte discharge is regulated by light and opsin-mediated phototransduction. *BMC Biology* **10,** 17. ISSN: 1741-7007. https://doi.org/10.1186/1741-7007-10-17 (2024) (Mar. 5, 2012).
45. Pang, R. & Fairhall, A. L. Fast and flexible sequence induction in spiking neural networks via rapid excitability changes. *eLife* **8** (eds Salinas, E., Marder, E. & Salinas, E.) Publisher: eLife Sciences Publications, Ltd, e44324. ISSN: 2050-084X. https://doi.org/10.7554/eLife.44324 (2022) (May 13, 2019).
46. Bosch, T. C. Understanding complex host-microbe interactions in Hydra. *Gut Microbes* **3.** Publisher: Taylor & Francis _eprint: https://doi.org/10.4161/gmic.20660, 345–351. ISSN: 1949-0976. https://doi.org/10.4161/gmic.20660 (2024) (July 14, 2012).
47. Klimovich, A. *et al.* Prototypical pacemaker neurons interact with the resident microbiota. *Proceedings of the National Academy of Sciences* **117.** Publisher: Proceedings of the National Academy of Sciences, 17854–17863. https://www.pnas.org/doi/10.1073/pnas.1920469117 (2022) (July 28, 2020).
48. Giez, C. *et al.* Multiple neuronal populations control the eating behavior in Hydra and are responsive to microbial signals. *Current Biology* **33,** 5288–5303.e6. ISSN: 09609822. https://linkinghub.elsevier.com/retrieve/pii/S0960982223014392 (2024) (Dec. 2023).
49. Murillo-Rincon, A. P. *et al.* Spontaneous body contractions are modulated by the microbiome of Hydra. *Scientific Reports* **7.** Number: 1 Publisher: Nature Publishing Group, 15937. ISSN: 2045-2322. https://www.nature.com/articles/s41598-017-16191-x (2022) (Nov. 21, 2017).
50. Nawroth, J. C., Giez, C., Klimovich, A., Kanso, E. & Bosch, T. C. Spontaneous body wall contractions stabilize the fluid microenvironment that shapes host–microbe associations. *eLife* **12** (eds Goldstein, R. E. & Walczak, A. M.) Publisher: eLife Sciences Publications, Ltd, e83637. ISSN: 2050-084X. https://doi.org/10.7554/eLife.83637 (2023) (July 3, 2023).

Appendix A

Additional data

A.1 Neural activity and body length in the regenerating animal

This is the neural activity extracted from the bisection experiments, arranged into separate figures for each animal. The pre-bisected animal's activity is placed at the top right corner and the the right column shows activity from the lower half as it regenerates over day-0, 1, 2 and 3 after bisection and the left column shows the same for the hypostomal half of the animal.

In each plot the RP network activity is in orange and CB in blue, with each bar representing a firing event of the subnetwork. The envelope on top of it represents the instantaneous rate obtained by convolving the spiketrain with a gaussian kernel. In black superimposed on these neural activity plots is the relative length of the body column of the animal obtained by summing lengths of segments along the midline (see methods).

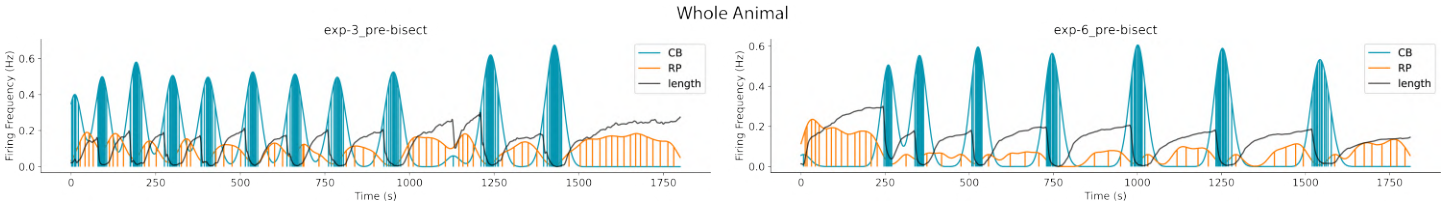

Fig. A.1. Neural activity and body length from recordings of the whole animal.

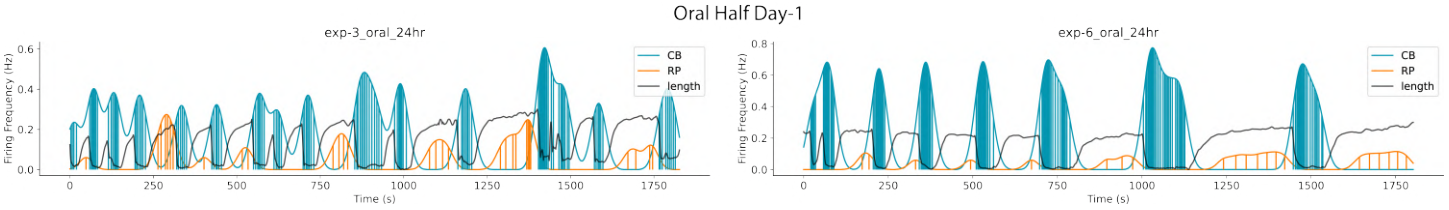

Fig. A.2. Neural activity and body length from recordings of the regenerating oral half - day-1.

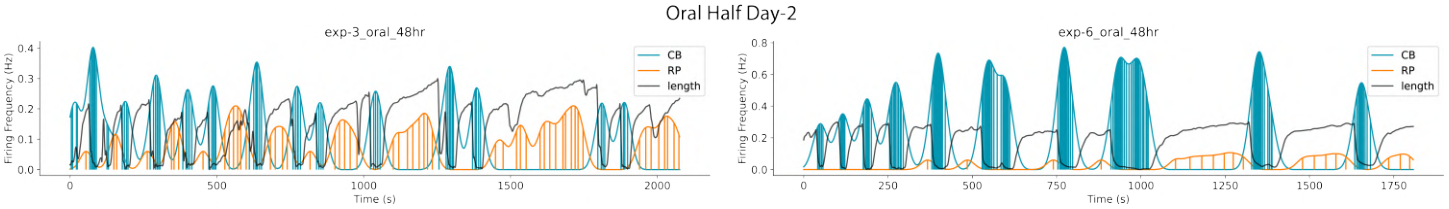

Fig. A.3. Neural activity and body length from recordings of the regenerating oral half - day-2.

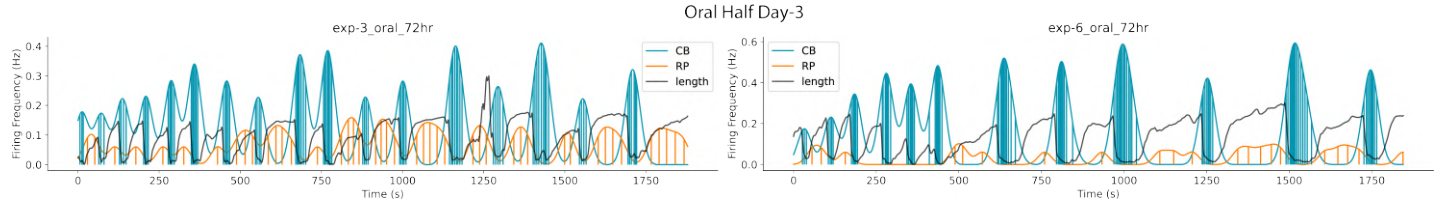

Fig. A.4. Neural activity and body length from recordings of the regenerating oral half - day-3.

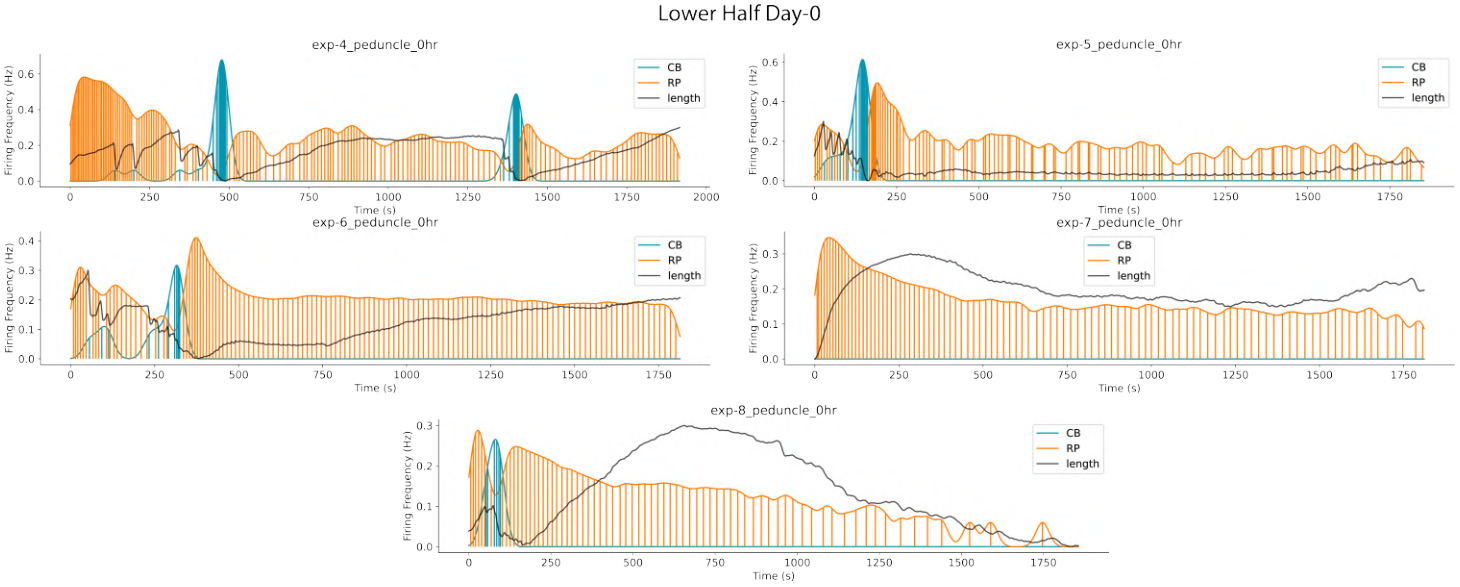

Fig. A.5. Neural activity and body length from recordings of the regenerating lower half - day-0.

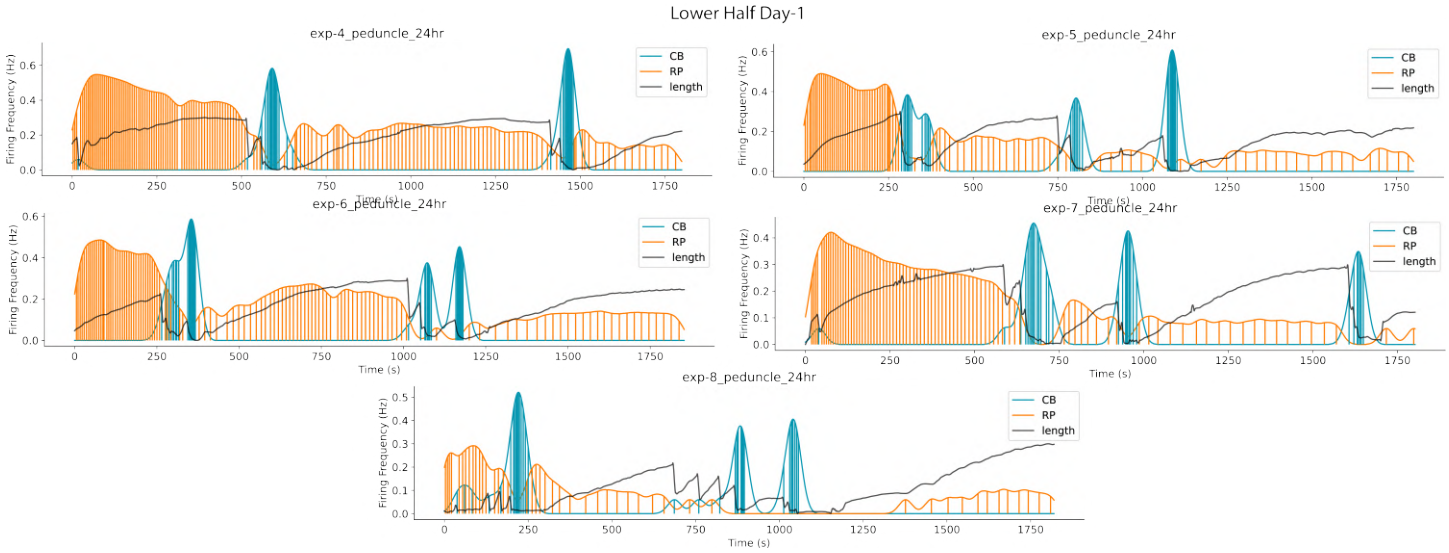

Fig. A.6. Neural activity and body length from recordings of the regenerating lower half - day-1.

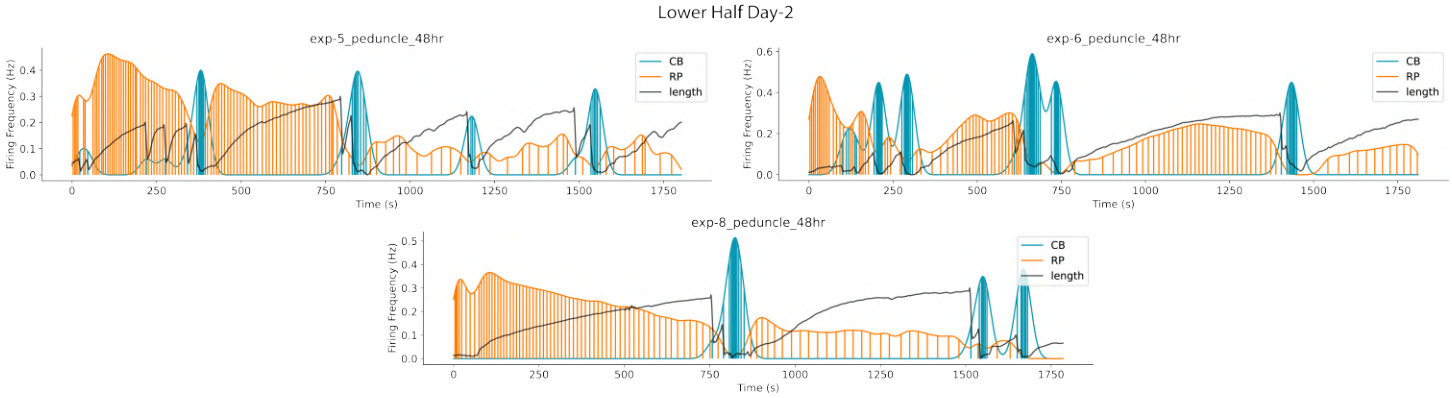

Fig. A.7. Neural activity and body length from recordings of the regenerating lower half - day-2.

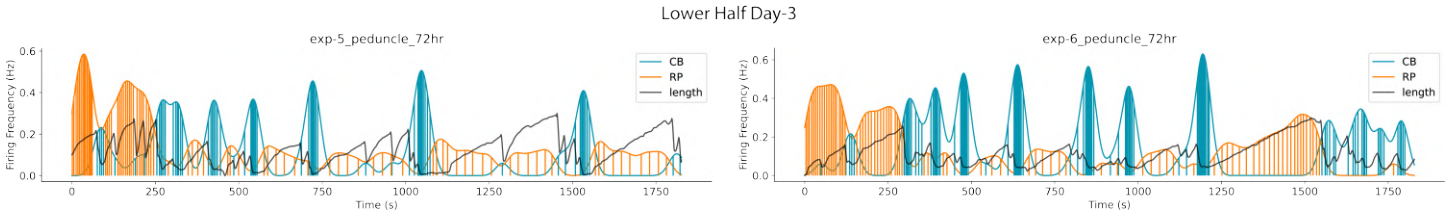

Fig. A.8. Neural activity and body length from recordings of the regenerating lower half - day-3.

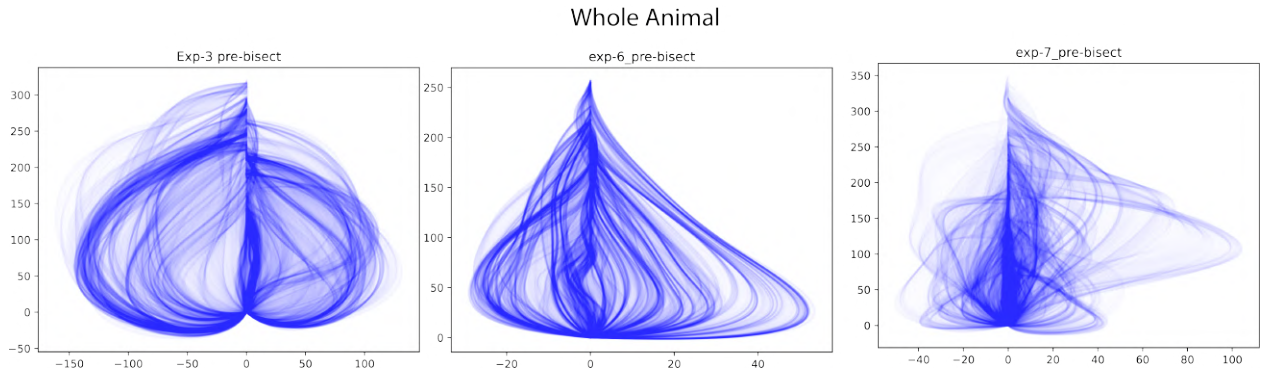

Fig. A.9. Hydra mid-line superimposed in time, from videos of the whole animal.

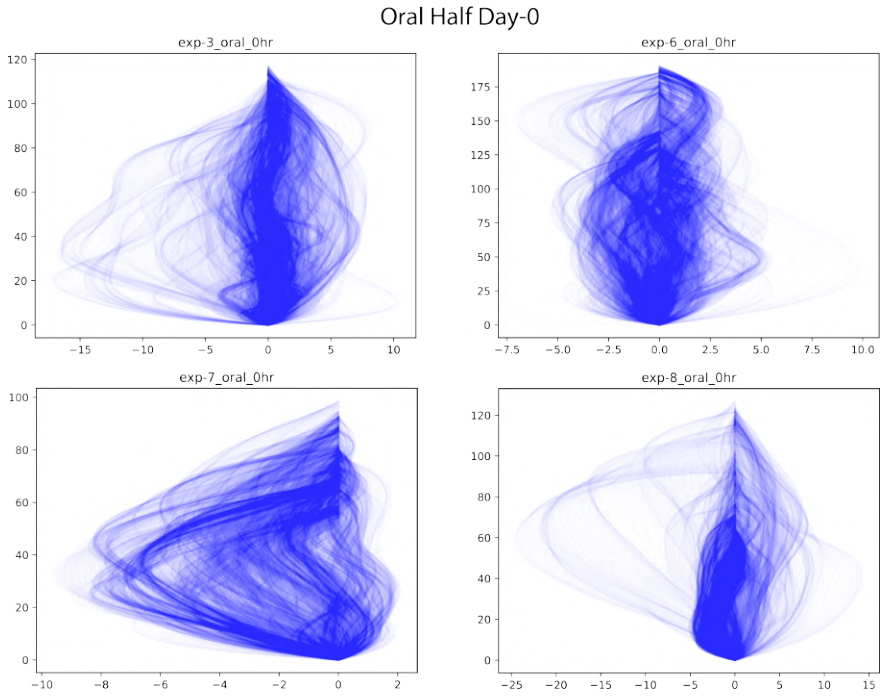

Fig. A.10. Hydra mid-line superimposed in time, from videos of the regenerating oral half, day-0.

A.2 Bending Dynamics

We visualize bending state by plotting the interpolated midline obtained by keypoint tracking from the videos of the behaving animal. Here are the plots from the whole animal and regenerating halves from our dataset organized by state of the animal.

Each plot shows the midline of the animal interpolated from keypoints tracked along its body using the pose estimation tool DeepLabCut (see methods). The midline is superimposed in time over the recording interval on the 2D x-y plane, with the foot end fixed to the origin and the midline rotated such that the foot-head axis remains aligned to the positive y-axis in the plot. The resulting plot with its left and right curves shows the bending behavior of the animal, with opacity indicating time density of a particular pose.

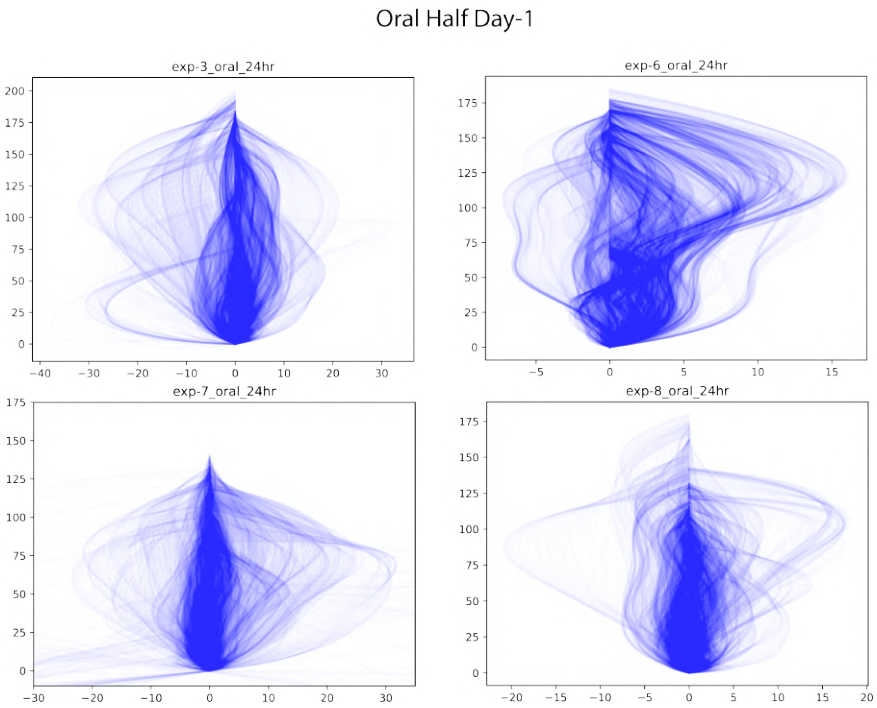

Fig. A.11. Hydra mid-line superimposed in time, from videos of the regenerating oral half, day-1.

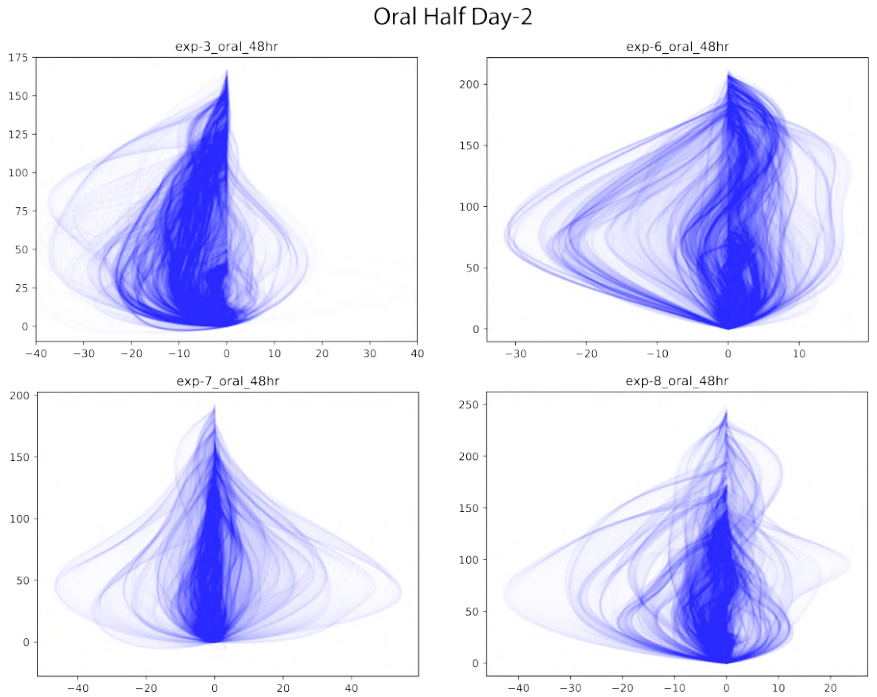

Fig. A.12. Hydra mid-line superimposed in time, from videos of the regenerating oral half, day-2.

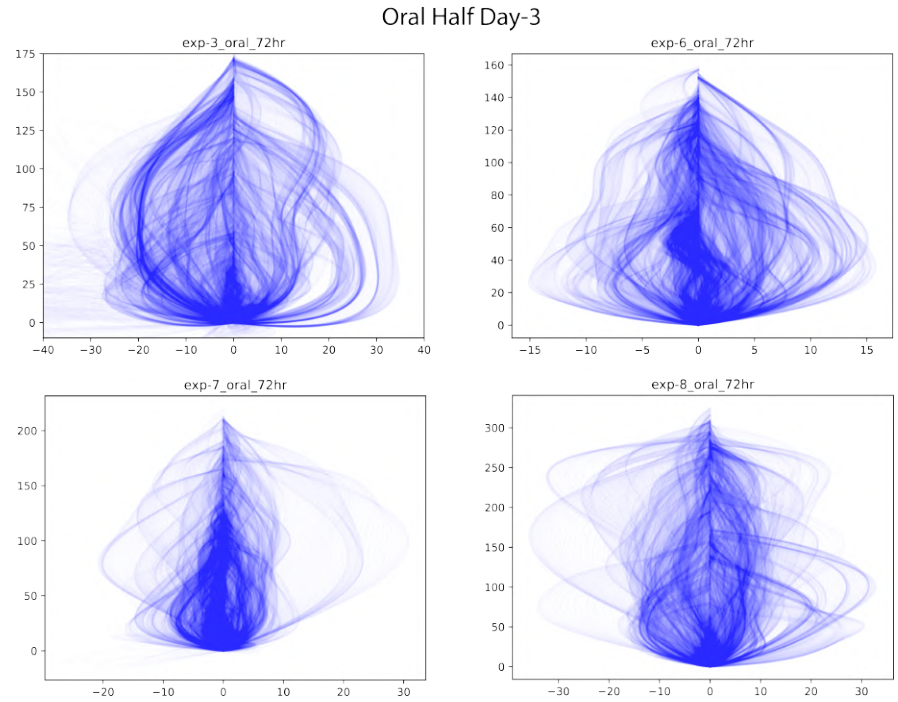

Fig. A.13. Hydra mid-line superimposed in time, from videos of the regenerating oral half, day-3.

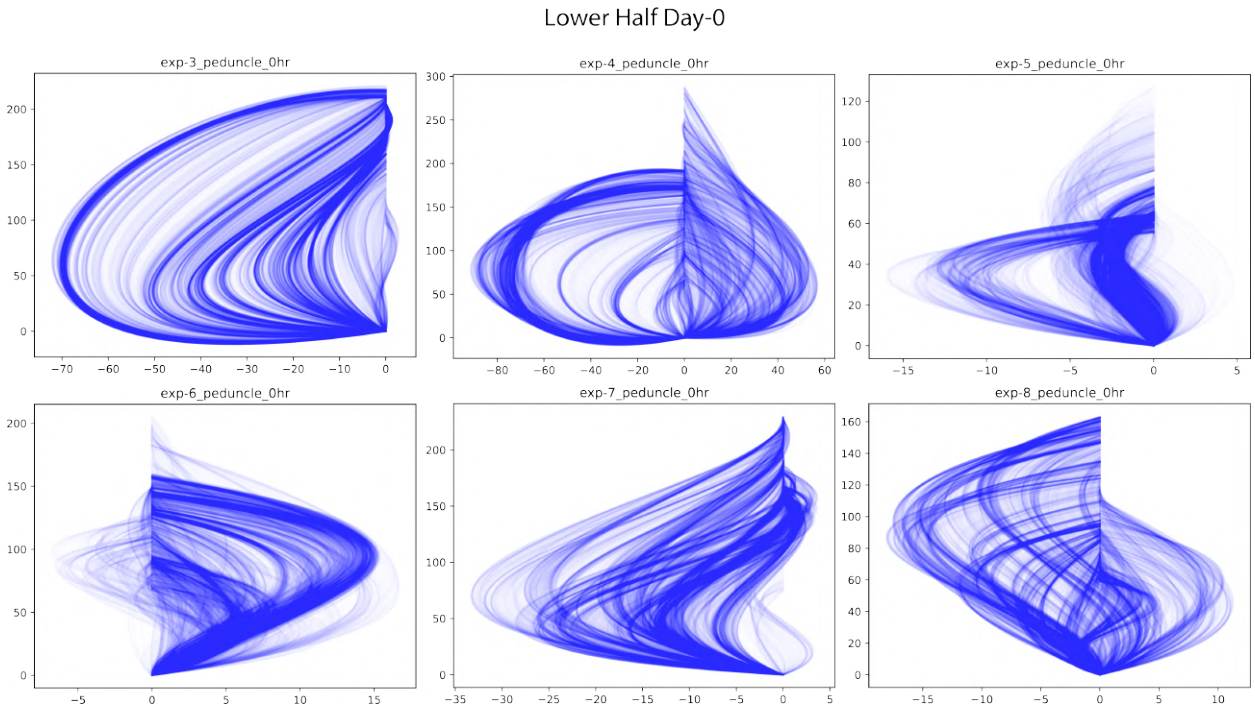

Fig. A.14. Hydra mid-line superimposed in time, from videos of the regenerating lower half, day-0.

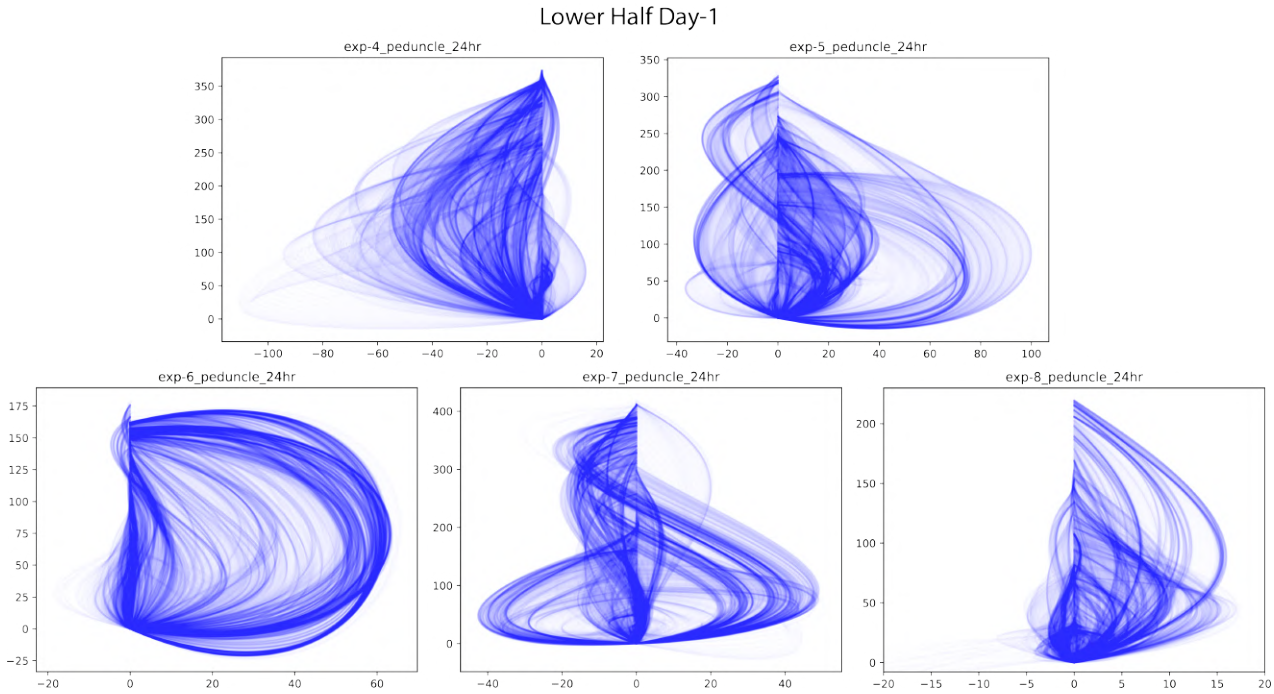

Fig. A.15. Hydra mid-line superimposed in time, from videos of the regenerating oral half, day-1.

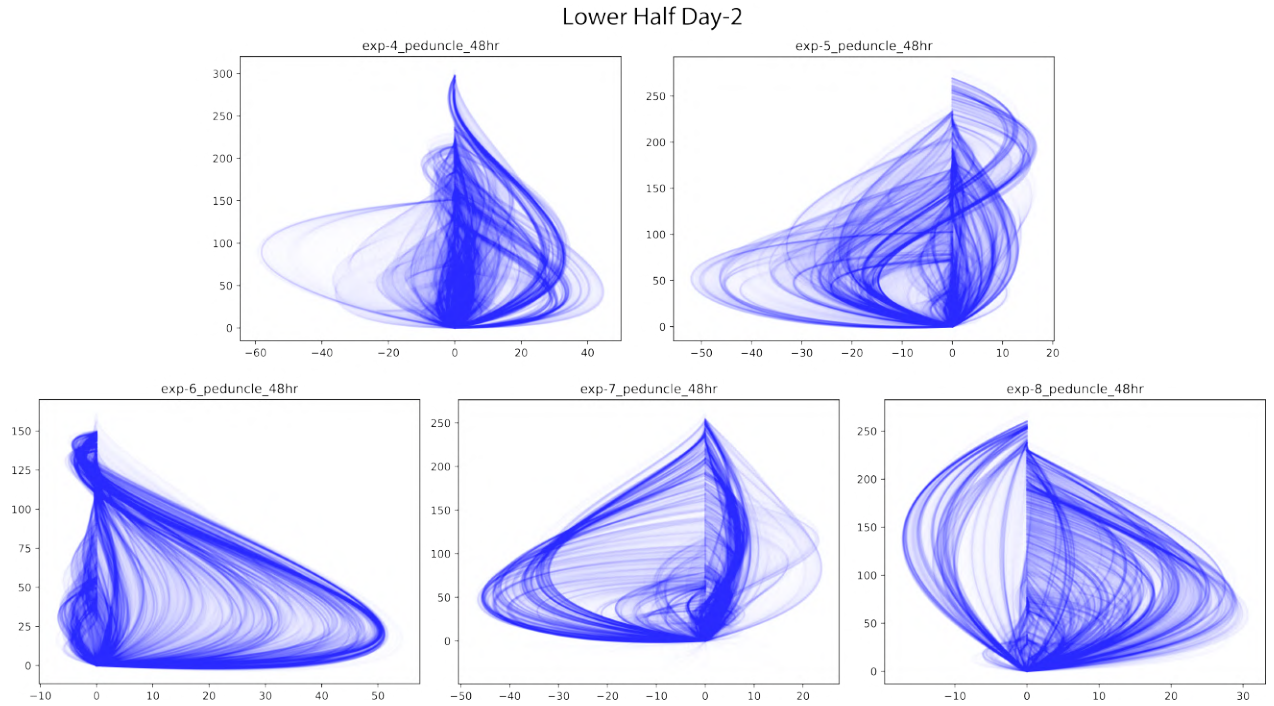

Fig. A.16. Hydra mid-line superimposed in time, from videos of the regenerating oral half, day-2.

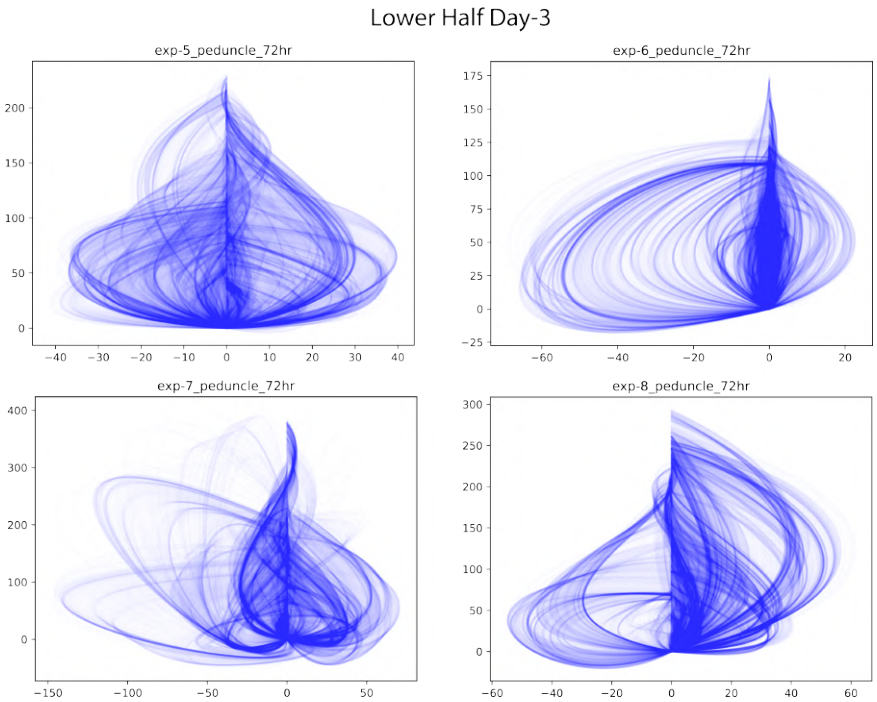

Fig. A.17. Hydra mid-line superimposed in time, from videos of the regenerating oral half, day-3.